Hierarchy of models for meandering rivers and related morphodynamic processes

HIERARCHY OF MODELS FOR MEANDERING RIVERS AND RELATED MORPHODYNAMIC PROCESSES

C. Camporeale,[1] P. Perona,[2] A. Porporato,[3] and L. Ridolfi[1]

Received 23 September 2005; revised 31 March 2006; accepted 10 October 2006; published 22 February 2007.

[1] We review the importance of the physical mechanisms involved in river meandering by comparing some existing linear models and extensions thereof. Such models are hierarchically derived from a common and general mathematical framework and then analyzed with a detailed discussion of the physical processes and relevant hypotheses that are involved. Experiments and field data are also used to discuss the related morphodynamic processes. The analysis of the models shows the importance of the closure of secondary currents especially in the modeling of eddy viscosity. This aspect confirms the usefulness of using simplified models for some practical applications, provided the secondary currents are modeled in detail. On the other hand, the free response of the sediments, the phase lag of secondary currents, and the momentum redistribution due to the coupling between the main and the transverse flow are shown to be less relevant. Hence the second-order models, which neglect the effect of superelevation induced by the topography-driven lateral flow on the longitudinal flow, can reasonably be considered a good approximation for both predictive analysis and the computation of the resonant conditions. Finally, the analysis of higher harmonics suggests that the multilobed pattern can intrinsically be present in both second- and fourth-order models.

Citation: Camporeale, C., P. Perona, A. Porporato, and L. Ridolfi (2007), Hierarchy of models for meandering rivers and related morphodynamic processes, *Rev. Geophys.*, *45*, RG1001, doi:10.1029/2005RG000185.

1. INTRODUCTION

[2] River meanders are one of the most ubiquitous patterns in fluvial morphology [e.g., *Chitale*, 1970; *Allen*, 1984; *Howard*, 1992]. For many years the beauty and applicative importance of these nearly regular loops in river *planimetry* have attracted the interest of several researchers in fluid mechanics and morphodynamics [*Ikeda and Parker*, 1989; *Seminara*, 1998, 2006], geomorphology [*Allen*, 1984], river engineering [*Jansen et al.*, 1979; *Elliott*, 1984], riparian ecology [*Salo et al.*, 1986], and petroleum engineering [*Swanson*, 1993]. (Italicized terms are defined in the glossary, after the main text.)

[3] From a physical point of view, meandering rivers form a dynamical system far from equilibrium, which, in its continuous evolution, exhibits some kind of statistical stationarity [*Cross and Hohenberg*, 1993; *Liverpool and Edwards*, 1995; *Stølum*, 1996; *Camporeale et al.*, 2005]. The river evolution is driven by fluid dynamic and morphodynamic processes, which cause lateral bank erosion and the continuous migration of meanders, as well as by sporadic *cutoffs* that prevent self-intersections of the river and produce sudden reductions in river length and sinuosity (see Figure 1). These internal dynamics are usually forced by external deterministic or stochastic factors, with different temporal and spatial scales, due to hydrological and riparian processes as well as to pedological, geological, and anthropic constraints. In the present review, attention is focused on the mathematical modeling of the fluid dynamic and morphodynamic processes that are responsible for the short-term evolution of rivers. We will also show how such mathematical models can be coupled with the cutoff dynamics and different types of external forcing to investigate the long-term evolution of meandering rivers.

[4] Historically speaking, the study of meandering rivers has followed two interrelated paths: a geomorphologic approach and a fluid dynamic approach. The geomorphologic approach, through fundamental field studies [e.g., *Leopold and Wolman*, 1960; *Kinoshita*, 1961; *Allen*, 1965; *Chitale*, 1970; *Nanson and Hickin*, 1983; *Carson and Lapointe*, 1983; *Thorne and Furbish*, 1995] and laboratory experiments [e.g., *Friedkin*, 1945; *Rozowskij*, 1957; *Zimmerman and Kennedy*, 1966; *Kinoshita and*

[1]Dipartimento di Idraulica, Trasporti ed Infrastrutture Civili and Idraulica e Ambiente, Water and Environment Research Center, Politecnico di Torino, Torino, Italy
[2]Institute of Hydromechanics and Water Resources Management, Eidgenossische Technische Hochschule Zurich, Zurich, Switzerland
[3]Department of Civil and Environmental Engineering, Duke University, Durham, North Carolina, USA

8755-1209/07/2005RG000185$15.00
Paper number 2005RG000185

Figure 1. An aerial photograph of the Colville River (Alaska). Enlargement and continuous migration of meanders as well as the formation of cutoffs can be observed.

Miwa, 1974; *Whiting and Dietrich*, 1993a, 1993b], has described the main characteristics of meanders and offered valuable empirical relationships on the planimetric features of meanders and river bed forms. The fluid mechanic approach has focused on the mathematical modeling of the physical mechanisms governing the meandering dynamics. The pioneering works of *Van Bendegom* [1947] and *Engelund* [1974] on the flow field and bed topography in a bend were followed by several important contributions that elucidated some key fluid dynamic aspects of river meandering. In particular, *Ikeda et al.* [1981] proposed the first model of the evolution of single reach of river bends by linking the flow field and the erosion rate; *Parker et al.* [1982, 1983] described the downstream migration of meanders and the occurrence of third-order harmonics in Kinoshita's curve; *Blondeaux and Seminara* [1985] clarified the link between the bend and alternate *bar* dynamics and pointed out their possible resonance; *Kalkwijk and De Vriend* [1980], *Kitanidis and Kennedy* [1984], and *Johannesson and Parker* [1989b] investigated the role of secondary currents; *Struiksma et al.* [1985] observed and modeled the *overdeepening phenomena*; *Tubino and Seminara* [1990] investigated the nonlinear interaction between bars and bends; and *Zolezzi and Seminara* [2001] pointed out the upstream propagating influence.

[5] After 3 decades of conspicuous efforts the scientific community has produced a number of different models of increasing detail and complexity. On one hand, the linear [e.g., *Ikeda et al.*, 1981; *Blondeaux and Seminara*, 1985; *Struiksma et al.*, 1985; *Odgaard*, 1986; *Crosato*, 1987; *Johannesson and Parker*, 1989a; *Zolezzi and Seminara*, 2001] and weakly nonlinear [*Seminara and Tubino*, 1992] models are strictly valid only for low curvatures of the river axis and slowly varying bed topography [*Seminara and Solari*, 1998] far from resonant conditions. However, because of their analytical solutions and their good agreement with observed river evolution [*Imran et al.*, 1999], they have been extensively used for both theoretical and numerical investigations of river morphodynamics [e.g., *Howard*, 1984; *Stølum*, 1996; *Sun et al.*, 1996, 2001a; *Seminara et al.*, 2001; *Edwards and Smith*, 2002; *Camporeale et al.*, 2005; *Camporeale and Ridolfi*, 2006; *Lanzoni et al.*, 2006]. On the other hand, fully nonlinear models [*Smith and McLean*, 1984; *Olsen*, 1987; *Nelson and Smith*, 1989b; *Shimizu et al.*, 1992; *Mosselman*, 1991, 1998; *Imran et al.*, 1999; *Duan et al.*, 2001; *Darby et al.*, 2002; *Blanckaert and De Vriend*, 2003] have less geometric restrictions and provide a better quantitative resolution of the flow, but they require a more demanding computational effort.

[6] Despite the advances produced by these various models, their formulations are difficult to compare (the formalisms are often different), and it is hard to evaluate what the effective role played by different modeling approximations is or whether the increasing modeling complexity is justified by the results. Apart from the work by *Parker and Johannesson* [1989], who performed a partial comparison between some models but focusing essentially on the resonance, overdeepening, and the dynamics of the secondary currents, no other comparative assessment has been published so far. For these reasons the main objective of the present work is to review the fundamental morphodynamic mechanisms that govern the meandering dynamics and to formulate a general framework from which the previously proposed linear models can be hierarchically derived and

then critically compared according to their hypotheses and their level of detail in the description of the various physical processes. In this manner the main models are obtained in cascade through a series of subsequent simplifications. We also derive some extensions of the existing theories that are useful for model intercomparison and for understanding the role of some physical processes involved in meandering dynamics. Finally, a comparison with a real case of meander evolution allows the role of the different model hypotheses to be highlighted.

[7] We have focused on linear theories as they allow one to take into account all the key processes that govern meandering dynamics but, at the same time, to maintain analytical tractability. Many fundamental conceptual results are thus obtained without the need of numerical simulations. However, in order to verify the reliability of the linear models we also derive a nonlinear version for each level of morphodynamic simplification and compare them with the correspondent linear models. To this aim we have extended the nonlinear iterative procedure by *Imran et al.* [1999] to the equation of sediment mass continuity.

[8] Particular attention is devoted to the models of *Ikeda et al.* [1981], *Johannesson and Parker* [1989a], and *Zolezzi and Seminara* [2001], hereinafter referred to as IPS, JP, and ZS, respectively, as they represent key steps in the comprehension and modeling of meandering dynamics. These models form the skeleton of our work, and we will refer to them when discussing other existing linear models [e.g., *Howard*, 1984; *Struiksma et al.*, 1985; *Odgaard*, 1986; *Crosato*, 1987; *Bridge*, 1992]. The IPS and JP models have been widely used in numerical simulations of river evolution [e.g., *Howard*, 1992; *Stølum*, 1996; *Sun et al.*, 1996, 2001a], while the ZS model is more detailed and encompasses all the principal morphodynamic mechanisms (for this reason, ZS is used here as the reference model, and its notation is extended to other models). Other linear models that focus on bank erosion and on how soil properties and riparian vegetation influence bank geotechnical characteristics are not discussed here [e.g., *Lancaster and Bras*, 2002; *Richardson*, 2002]. Although these models are interesting, they are not completely physically based, and as such they are not capable of describing the complex interactions that exist among bed topography, flow field, and sediment transport. As far as the role of bank erosion is concerned, mention is made here only of the refined two-dimensional (2-D) nonlinear models by *Darby et al.* [2002] and *Duan and Julien* [2005], where both fluid dynamic and geotechnical aspects are modeled in detail.

[9] It should be noted that all the previously mentioned models share two important basic assumptions: (1) The river discharge is always assumed to be constant and usually equal to the mean annual or bankfull value, and (2) the shallow water approximation allows the flow field to be solved using a 2-D (or quasi-three-dimensional) depth-averaged scheme. Although the former assumptions can result in rather crude approximations, only in very few studies have they been at least in part relaxed. In particular, in the work of *Howard and Hemberger* [1991] the IPS model was forced with temporally varying discharges extracted from a lognormal distribution. The authors did not observe a relevant change in the statistical behavior of the river planimetry with respect to the case with a constant discharge equal to the mean value. However, the determination of the formative discharge for the meandering patterns still remains an open question, since it does not necessarily coincide with the dominant geomorphic discharge for the hydraulic geometry proposed by *Wolman and Miller* [1960].

[10] The problem of resolving the flow field using a three-dimensional (3-D) rather than a 2-D approach has received much more attention, especially from a numerical point of view [*Shimizu et al.*, 1990; *Ye and McCorquodale*, 1998; *Ferguson et al.*, 2003; *Olsen*, 2003; *Wilson et al.*, 2003; *Blanckaert and De Vriend*, 2004; *Rüther and Olsen*, 2005], although the linear analytical treatment by *Seminara and Tubino* [1989] should also be mentioned. The main result is that the 2-D scheme cannot give a correct description of the flow field when either the bend curvature is high or the aspect ratio is too low, which corresponds to the breakdown of the shallow water approximation. In these circumstances the numerical solution of the 3-D helicoidal motion becomes essential for modeling meandering dynamics.

[11] To date, the necessary high computational efforts limit the use of full 3-D models to simple geometries with sharp bends and hinder the simulation of the planimetric evolution of rivers, as testified by the comparisons with experimental data that are restricted to channels with fixed banks. However, the increasing advances in computer science suggest that the adoption of powerful computational fluid dynamics tools, such as direct numeric simulation (DNS), large eddy simulation (LES), or k-ε models, will produce important contributions in the context of the emerging discipline of numerical morphodynamics [e.g., *Keylock et al.*, 2005].

[12] The paper is organized as follows. Section 2 gives a detailed qualitative description of the morphodynamic processes involved in meandering dynamics, while section 3 is devoted to the general mathematical modeling of the meandering dynamics and to presenting a method for the nonlinear solution of the morphodynamic problem. In section 4, the different linear models are derived from the same general formalism and discussed according to their level of approximation. When deducing the linear models, some extensions of the existing theories are also derived that are useful for the comparison of the models and for understanding the role of some physical processes involved in meandering dynamics. The various linear models are compared in section 5 by analyzing their free and forced response separately, being the curvature the forcing of the system. The experimental verification of the longitudinal flow field is presented in section 6, while the behavior of each model is discussed in section 7 for some typical meander configurations and a field case in order to evaluate the quantitative importance of the degree of refinement of each model. The role of some external forcings in long-term

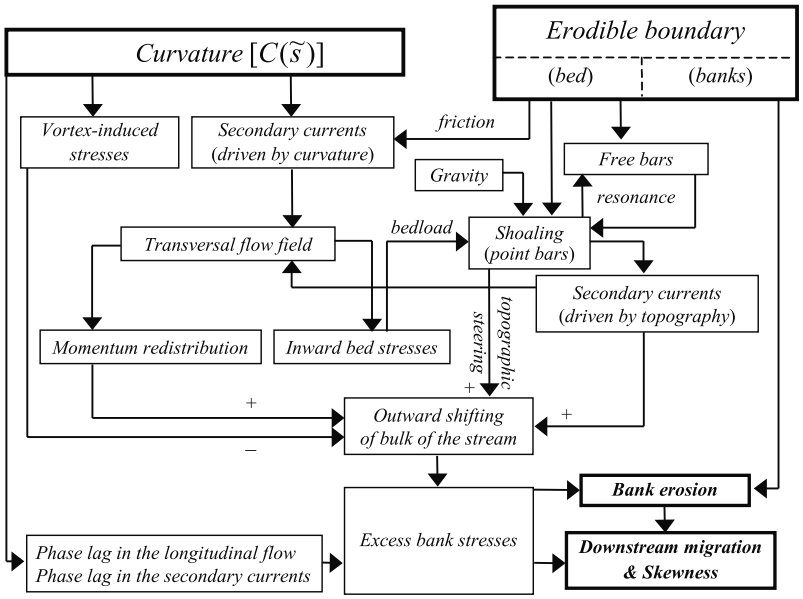

Figure 2. Scheme of the main processes involved in the meandering dynamics and their interactions.

dynamics is reviewed in section 8, and the conclusions follow in section 9. A brief glossary of the typical expressions herein adopted closes this review.

2. PHYSICAL PROCESSES

[13] We refer to the conceptual scheme of Figure 2 to describe the interrelationships among the physical processes that act in meandering rivers and to discuss their role in the context of the hierarchy of models that will be developed. Readers who are already familiar with the basic physics of meandering rivers may wish to skip to section 3. An orthogonal curvilinear reference system $\{\tilde{s}, \tilde{n}, \tilde{z}\}$, sketched in Figure 3, is used where $\tilde{s}$ is the longitudinal coordinate along the channel axis, $\tilde{n}$ is the transverse coordinate, and $\tilde{z}$ is the upward vertical coordinate. We also define the mean flow depth, $\tilde{D}_0$, and the channel width, $2\tilde{b}$.

[14] The two key elements necessary for meandering dynamics are the curvature, $C = C(\tilde{s})$, of the channel axis and the erodibility of the bed and banks. The longitudinal curvature has two direct effects on the stream: It induces additional shear stresses and drives the secondary currents. Assuming inviscid fluid and constant curvature, it is easy to see, from Euler's equations, the existence of a free irrotational vortex with transversal profiles of the streamwise velocity, $\tilde{U} = \tilde{U}(\tilde{n})$, and surface level of the flow, $\tilde{h} = \tilde{h}(\tilde{n})$ [e.g., *Henderson*, 1966; *Callander*, 1978]. Adding viscosity gives rise to shear stresses (i.e., vortex-induced stresses, Figure 2) that are responsible for the inside-bank erosion and contribute to straightening small-radius bends. The presence of friction on the bed also induces a vertical profile $\tilde{U} = \tilde{U}(\tilde{n}, \tilde{z})$. A tangential stress $\tilde{\tau}_{\tilde{z}\tilde{n}}$ is thus required to satisfy the momentum balance, and this, in turn, implies the formation of a streamwise secondary vorticity that produces the secondary currents (with vanishing net flux [*Seminara*, 1998]). The secondary currents cause a transversal flow field, which, in turn, produces inward bed stresses and a redistribution of the downstream momentum. This latter

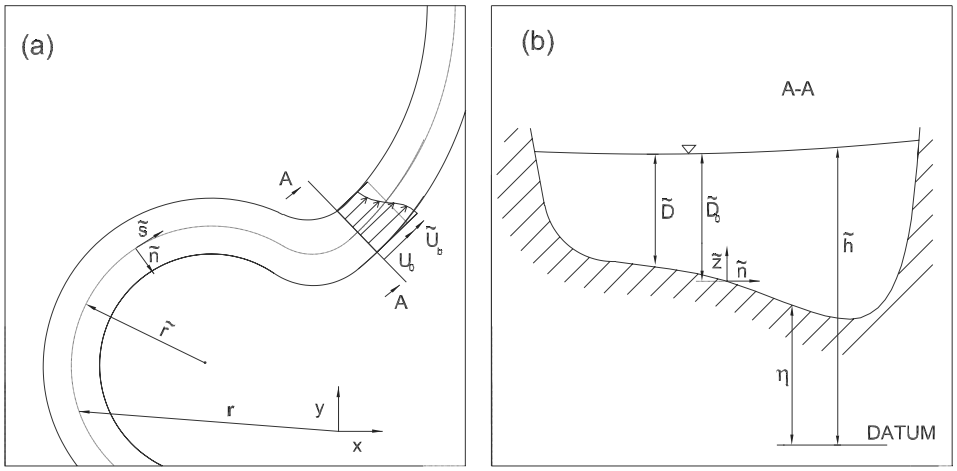

Figure 3. Scheme of the geometric variables: (a) planimetric and (b) section views.

gives rise to a shifting of the bulk of the stream toward the outside bank [*Kalkwijk and De Vriend*, 1980; *Johannesson and Parker*, 1989c] that is partially contrasted by the vortex-induced stresses. Moreover, the nonlinear feedback between the downstream velocity and the secondary cell deforms the vertical profile of the lateral flow, decreasing it in the upper part and increasing it in the lower part [*Blanckaert and De Vriend*, 2004].

[15] The second key element of meandering dynamics is the erodibility of the boundaries. The inward bed stresses, due to secondary currents, cause a transverse inward sediment transport, which deepens the riverbed at the out bank, produces a transversal shoaling of the bed, and induces the formation of point bars. This, in turn, shifts the bulk of the longitudinal flow outward (i.e., topographic steering [*Dietrich and Smith*, 1983]) and triggers a different type of lateral flow because of the bed topography (i.e., topography-induced lateral flow). These processes are generally more important than the aforementioned curvature-induced secondary currents [*Seminara*, 1998] and influence the transversal flow field inducing a further outward shift of the main flow (see Figure 2).

[16] Bed erodibility is also essential in the interactions between the curvature and the self-excited response of the bed planform [*Blondeaux and Seminara*, 1985]. While both low-sinuosity and high-sinuosity rivers have downstream migrating alternate perturbations, known as free bars [*Kinoshita and Miwa*, 1974; *Whiting and Dietrich*, 1993a], only in rivers with intermediate sinuosity can the nonlinear interactions between point bars and free bars suppress the growth of the latter forms [*Tubino and Seminara*, 1990]. The interaction between free response (i.e., alternate bars) and forced response (i.e., point bars) displays a resonant behavior when rivers have a particular aspect ratio β_R (where $\beta = \tilde{b}/\tilde{D}_0$) and wavelength L_R. In such conditions, nonmigrating and nonamplifying alternate bars reinforce the effect of the point bars so that the flow and bed perturbations peak [*Blondeaux and Seminara*, 1985]. Moreover, because of the feedback between morphodynamics and hydrodynamics on the bed stress distribution a curvilinear stream needs a longitudinal bed slope that is different from that of a straight stream to carry the same sediment bed load [*Seminara and Solari*, 1998].

[17] The streamwise variation of the channel curvature influences the longitudinal transport of momentum by inducing a streamwise phase lag between the planimetric curvature and the pattern of the flow field in the river. This lag, which depends on the frictional turbulent dissipation and is of the order of the channel width, controls the spatial memory of the downstream propagating influence [*Howard*, 1984; *Smith and McLean*, 1984] and is the reason for both the downstream *skewness* in the shape of the meander loops and the downstream planimetric migration [*Friedkin*, 1945; *Engelund*, 1974; *Dietrich et al.*, 1979; *Ikeda et al.*, 1981; *Parker et al.*, 1982]. Recently, *Zolezzi and Seminara* [2001] pointed out the existence of an upstream influence component that is capable, in particular conditions, of producing an upstream migration of meanders in agreement with some laboratory observations [*Garcia and Nino*, 1993; *Hasegawa et al.*, 1998]. Longitudinal variations in curvature also induce a phase lag in the pattern of the secondary currents [*Gottlieb*, 1976; *Kitanidis and Kennedy*, 1984; *Ikeda and Nishimura*, 1986; *Zhou et al.*, 1993]. This aspect, however, is of secondary importance, as it has a spatial scale of the order of the channel depth [*Johannesson and Parker*, 1989b; *Edwards and Smith*, 2002].

[18] The result of the aforementioned processes is the formation of excess bank stresses that are responsible for the lateral erosion of the outward bank and therefore for the meander evolution (see Figure 3). In particular, the planimetric evolution of meanders takes place in three stages: first, a marked downstream migration with a weak amplitude growth; second, an increased amplitude growth; and finally, a progressive decay in migration and growth until bend cutoff occurs [*Seminara*, 1998]. In this evolution the interplay of topographic steering, vortex-induced stresses, and curvature effects on the longitudinal bed slope gives rise to the fattening of the meander loops [*Langbein and Leopold*, 1966; *Parker et al.*, 1982, 1983; *Parker and Andrews*, 1986; *Seminara et al.*, 1994].

3. MATHEMATICAL FORMULATION

3.1. Basic Hypotheses

[19] Some basic hypotheses are necessary in order to obtain significant but mathematically tractable models. (1) The fluid is assumed to be incompressible and the flow to be fully turbulent, while the cohesion of the riverbed is neglected, and the river is assumed to maintain a constant width during lateral migration [*Friedkin*, 1945]. Although some works explored the influence of sediment heterogeneity [*Allen*, 1970; *Odgaard*, 1982; *Parker and Andrews*, 1985; *Ikeda et al.*, 1987; *Ikeda and Parker*, 1989; *Bridge*, 1992] and suspended sediment [*Seminara and Tubino*, 1985], these effects are generally neglected in meander models. (2) Since the typical vertical scale (i.e., the water depth $\tilde{D}_0$) is much smaller than the characteristic horizontal scale (i.e., the river half-width $\tilde{b}$), the vertical velocity component can be neglected, and a hydrostatic vertical pressure distribution can be adopted. Since this approximation of the shallow water theory [e.g., *Ligget*, 1994] is violated near the banks, because of the influence of the boundary layers, it is clear that the theory that will be developed is only valid in the central part of the stream (we will come back to this aspect in section 4.2). (3) It can be assumed that both the flow and bed topography instantaneously adjust to the planimetry, considering the process as quasi-stationary. It follows that the time dependence of the equations can be neglected [*De Vries*, 1965]. Evidently, such a hypothesis prevents the direct modeling of free-bar migration. (4) The last essential hypothesis concerns the assumption of a linear relationship, the so-called Partheniades type, between the rate of bank erosion and the ratio of the near-bank shear stress to the average boundary shear stress [*Partheniades*, 1965; *Partheniades and Paaswell*, 1970], which can be reexpressed [*Howard*, 1992] in terms

of a linear relationship between the bank erosion and excess near-bank velocity perturbation $\tilde{U}_b$ (see Figure 3). This assumption has been adopted in several models because of its simplicity [e.g., *Ikeda et al.*, 1981; *Parker et al.*, 1983; *Parker and Andrews*, 1986; *Johannesson and Parker*, 1989a; *Odgaard*, 1986], and it is justified by field observations [*Pizzuto and Meckelnburg*, 1989]. *Hasegawa* [1989] offered a possible theoretical justification of this linear relationship considering channels with noncohesive banks where the rate of bank line erosion is computed by the use of a bed load formula on the lateral bank. This justification was, however, criticized because bank cohesiveness alone could justify a linear Partheniades-type formula for bank erosion [*Mosselman and Crosato*, 1991].

3.2. Governing Equations

[20] Let us introduce the following dimensionless variables (see Figure 3)

$$(s,n)=\frac{(\tilde{s},\tilde{n})}{\tilde{b}},\qquad (u^*,v^*,w^*)=\frac{(\tilde{u},\tilde{v},\tilde{w})}{\tilde{U}_0}, \tag{1}$$

$$(h^*,\eta,D,z,d_s)=\frac{\left(\tilde{h},\tilde{\eta},\tilde{D},\tilde{z},\tilde{d}_s\right)}{\tilde{D}_0},\qquad C=\frac{\tilde{b}}{\tilde{r}}, \tag{2}$$

$$\nu_T=\frac{\tilde{\nu}_T}{\sqrt{C_f}\tilde{U}_0\tilde{D}_0},\qquad N=\frac{1}{1+nC},\qquad F_0=\frac{\tilde{U}_0}{\sqrt{g\tilde{D}_0}}, \tag{3}$$

$$\nu_0=\frac{\tilde{b}}{\tilde{R}_0},\qquad \mathbf{q}=\frac{\tilde{\mathbf{q}}}{\sqrt{\hat{\rho}\tilde{d}_s^3}},\qquad \boldsymbol{\tau}=\frac{\tilde{\boldsymbol{\tau}}}{\rho\tilde{U}_0^2},\qquad \mathbf{t}^*=\frac{\tilde{\boldsymbol{\tau}}}{\rho\hat{\rho}\tilde{d}_s}, \tag{4}$$

where $(\tilde{u},\ \tilde{v},\ \tilde{w})$ are the longitudinal, normal, and vertical velocity components, $\tilde{U}_0$ is the bulk velocity, $\tilde{D}(s,\ n)$ is the local flow depth, $\tilde{h}(s,\ n)$ is the free surface level, $\tilde{\eta}(s,\ n)$ is the bed elevation, $\tilde{d}_s$ is the average grain diameter, F_0 is the Froude number, ν_T is the dimensionless turbulent viscosity (C_f is the friction coefficient), $N(s)$ is the longitudinal metric coefficient, and C is the dimensionless curvature. Moreover, $\tilde{R}_0$ is the minimum radius of curvature in the river, $\tilde{\mathbf{q}}(s,\ n)=\{q_s,\ q_n\}$ is the volumetric bed load transport vector per unit width, $\hat{\rho}=g(\rho_s/\rho-1)$, ρ_s and ρ are the sediment and water densities, respectively, $\mathbf{t}^*=\{t_s,\ t_n\}$ is the dimensionless bed stress vector, $\tilde{\boldsymbol{\tau}}$ is the bed stress vector, and $\tilde{I}$ is the overall slope of the bed. We also introduce $\chi_0=\beta\sqrt{C_f}$ and $\chi_1=\beta C_f$ and note that the uniform flow implies $g\tilde{D}_0\tilde{I}=C_f\tilde{U}_0^2$ [*Henderson*, 1966]. Hence, as $\tilde{h}_s$ is the reference elevation and $\tilde{h}$ is the elevation with respect to the reference level at the river head, it follows that $\tilde{h}_s=\tilde{h}-\tilde{I}\,\tilde{s}$ or, in dimensionless variables, $h_s^*=h^*-\chi_1F_0^2s$.

[21] The starting point of the modeling is represented by Reynolds' equations for the momentum and mass conservation, written in orthogonal coordinates for the steady flow,

$$Nu_{,s}^{*2}+(u^*v^*)_{,n}+2NCu^*v^*+N\left(F_0^{-2}h_{,s}^*-\chi_1\right)-\chi_0\left(\nu_Tu_{,z}^*\right)_{,z}=0, \tag{5}$$

$$N(u^*v^*)_{,s}+v_{,n}^{*2}+NC\left(v^{*2}-u^{*2}\right)+F_0^{-2}h_{,n}^*-\chi_0\left(\nu_Tv_{,z}^*\right)_{,z}=0, \tag{6}$$

$$Nu_{,s}^*+v_{,n}^*+NCv^*=0, \tag{7}$$

where the comma indicates the partial derivative. On the basis of the primary approximation of the shallow water theory the first step is the depth averaging of equations (5)–(7). For this purpose the velocity components are decomposed as [*Kalkwijk and De Vriend*, 1980; *Smith and McLean*, 1984]

$$u^*=U(n,s)\mathcal{F}(\zeta) \tag{8a}$$

$$v^*=v_0(\zeta,n,s)+V(n,s)\mathcal{F}(\zeta), \tag{8b}$$

where $\zeta(s,\ n)=(z-\eta)/D$ and $\mathcal{F}(\zeta)$ is a suitable vertical profile. In the longitudinal velocity, $U=U(n,\ s)$ is simply the depth average of u^*, while the normal velocity component, v^*, is decomposed into a contribution because of the centrifugally induced velocity (the secondary current v_0), which has a vertical distribution with zero average, and a second contribution induced by the topographic and inertial effects, with a nonvanishing depth average $V(n,\ s)$. Note that (1) the same vertical profile $\mathcal{F}(\zeta)$ is used for both u^* and v^* and (2) $\mathcal{F}(\zeta)$ does not depend on the local position $(s,\ n)$. These assumptions are rigorously justified only in the linear approach, as they preclude the occurrence of the external deformation in the vertical profile of the lateral flow. However, such a hypothesis can also be reasonably formulated in the nonlinear case, as pointed out by *Tubino and Seminara* [1990] and as assessed here in section 6 using experimental data. Moreover, following a recent numerical result by *Blanckaert and De Vriend* [2003], this nonlinear feedback can be considered negligible if $\mathcal{B}\le 0.4$, with $\mathcal{B}=C_f^{-0.275}(\nu_0/\beta)^{0.5}(\alpha_s+1)$ and α_s is a parameter within the interval $[-1,\ 1]$. This condition is generally satisfied in real rivers without sharp bends and assuming $d_s=[10^{-3}\div 10^{-1}]$ and β is greater than 6.

[22] Adopting the velocity decompositions (8), the no-slip condition at the bottom, the no-stress condition at the free surface, and introducing the term $H=F_0^{-2}h^*-\beta C_fs$, one obtains the depth-averaged two-dimensional equations for shallow waters [*Johannesson and Parker*, 1989a; *Zolezzi and Seminara*, 2001; *Blanckaert and De Vriend*, 2003]

$$NUU_{,s}+VU_{,n}+NCU(V+2\varphi)+NH_{,s}+\beta\frac{\tau_s}{D}+\frac{1}{D}(UD\varphi)_{,n}=0 \tag{9}$$

$$NUV_{,s} + VV_{,n} + H_{,n} + \beta\frac{\tau_n}{D} + \frac{N}{D}(DU\varphi)_{,s} + \frac{2}{D}(VD\varphi)_{,n} + \frac{1}{D}(\varphi_1 D)_{,n} + NC\varphi_2 = 0, \quad (10)$$

which have to be coupled to the continuity equations for the water and bed sediment [*Exner*, 1925], respectively,

$$N(DU)_{,s} + (DV)_{,n} + NCDV = 0 \quad (11)$$

$$Nq_{s,s} + q_{n,n} + NCq_n = 0. \quad (12)$$

Equations (9)–(11) imply $\langle \mathcal{F}^2 \rangle \simeq \langle \mathcal{F} \rangle = 1$, $\varphi = \langle \mathcal{F} v_0 \rangle$, $\varphi_1 = \langle v_0^2 \rangle$, where $\langle \ldots \rangle = \int_{\zeta_0}^{1} (\ldots) d\zeta$ and ζ_0 is the vertical position at which the no-slip condition is set, and $\varphi_2 = 2V\varphi - U^2 + \varphi_1$. The term φ is the momentum redistribution term due to the interaction between the secondary currents and the main flow, and φ_1 derives from the lateral flux of the secondary currents.

[23] Finally, the following boundary and integral conditions are imposed

$$V = q_n = 0 \qquad (n = \pm 1), \quad (13)$$

$$\int_{-1}^{1} UDdn = 2, \quad (14a)$$

$$\int_0^{L_m} \int_{-1}^{1} (h^* - D) dnds = const \quad (14b)$$

where (13) is the zero-net-flux condition between the center and the sidewall layers that imposes no sediment transport across the sidewalls and (14a) and (14b) ensure that the water discharge and the average bed slope are not influenced by perturbations in flow and topography (L_m is a typical dimensionless wavelength). Equations (9)–(12), with boundary conditions (13) and (14), describe the morphodynamics of meandering rivers under the shallow water assumption and in the absence of sharp bends.

3.3. Constitutive Relationships

[24] System (9)–(12) needs closure relationships for the terms $\boldsymbol{\tau}$, $\mathbf{q}$, and v_0. Since a rigorous development would be prohibitive as it would require one to describe both the vertical turbulent structure and the dynamics of the coherent structures near the bed [*Robinson*, 1991; *Nezu and Nakagawa*, 1993], semiempirical closure schemes are usually adopted in morphodynamic modeling for simplicity. The main goal of river meandering morphodynamics is not in fact to describe the flow-bed interactions that occur at a microscale or mesoscale (e.g., ripples and dunes) but rather to focus on macroscale bed forms, i.e., the development of bars that have typical length scales of the order of the channel width [*Colombini et al.*, 1987]. For this reason, flow separations at the bed are not modeled as the flow field is assumed to be slowly varying. It follows that the dimensionless bed stress vector, $\boldsymbol{\tau}$, is aligned with the near bed velocity vector and can be expressed through a local friction coefficient C_f according to [*Tubino and Seminara*, 1990]

$$\tau_s = C_f |\mathbf{U}| U \quad (15a)$$

$$\tau_n = C_f |\mathbf{U}| \left(V + \frac{v_0(\zeta_0)}{\mathcal{F}(\zeta_0)} \right). \quad (15b)$$

[25] Exner equation (12) needs a closure relationship for the components of bed load transport, $\mathbf{q}$, which, under steady conditions and for bed slopes much smaller than the friction angle, can be modeled by a linear dependence on the bed horizontal gradient [*Van Bendegom*, 1947; *Kikkawa et al.*, 1976; *Ikeda*, 1982; *Nelson and Smith*, 1989a; *Kovacs and Parker*, 1994; *Talmon et al.*, 1995]. The dynamic equilibrium of the bed sediment, written in an orthogonal reference system (s, n), gives the following relationship [*Zolezzi and Seminara*, 1998]

$$q_i = q \left[\frac{t_i^*}{t^*} - \frac{1}{\beta} \left(\frac{t_i^{*2}}{t^{*2}} \frac{t_c^*}{\mu q_0} q_{,t^*}|_0 + \frac{t_j^{*2}}{t^{*2}} \frac{r}{\sqrt{t_0^*}} \right) \eta_{,i} + \left(\frac{r}{\sqrt{t_0^*}} - \frac{t_c^*}{\mu q_0} q_{,t^*}|_0 \right) \frac{t_i^* t_j^*}{\beta t^{*2}} \eta_{,j} \right], \quad (16)$$

where the longitudinal (or transversal) component of bed load transport, q_s (or q_n), is obtained setting $(i, j) = (s, n)$ (or $(i, j) = (n, s)$), while $t^* = |\mathbf{t}^*|$, t_0^* is the Shields stress, t_c^* is the critical Shield stress, μ is the dynamic friction coefficient, $q = |\mathbf{q}|$ is the dimensionless bed load transport (q_0 refers to uniform flow), and r is a coefficient in the range 0.5–0.6 [*Engelund*, 1981]. *Tubino and Seminara* [1990] pointed out the empirical character of (16) that only justifies its adoption in a linear context, although in practice the nonlinearities neglected in (16) are weak. Thus in the following, since in sinuous rivers $\partial\eta/\partial s \ll \partial\eta/\partial n$, the effect of the longitudinal bed slope is neglected.

[26] A suitable closure for the term $v_0(\zeta, n, s)$, which represents the vertical structure of the secondary currents, is needed for the evaluation of terms φ, φ_1, and φ_2 in equations (9)–(10) and for the computation of the bed stress in the sediment equation (16). For this purpose we refer to the method of *Zolezzi and Seminara* [2001], who extended the iterative analysis of *Seminara and Solari* [1998] to channels with variable curvature but neglected the lateral variation of the vertical structure of v_0. The method is based on Reynolds' equation (6), written for the transversal flow, and it adopts an eddy viscosity profile of the form $\nu_T = UD\Gamma(\zeta)$, where $\Gamma(\zeta)$ is a slowly varying function that will be defined later. A decomposition similar to that used for the velocity components (e.g., equation (8b)) is employed for the water surface elevation, i.e., $h^* = \hat{H}(n, s) + h_0(n, s)$, where h_0 is the centrifugally induced term and $\hat{H}$ is the term due to the topographic and inertial effects. Both the influence of the metric coefficient, N, and the effect of the spatial variation

of V on the evaluation of v_0 are neglected, so that $N = 1$ and $\hat{H} = 1$. It should be noticed that the latter assumption is only adopted for the computation of the secondary currents but can be relaxed for the solution of the full morphodynamic problem, e.g., the evaluation of the variables U, V, D, and H. This point will be further discussed in section 4.

[27] Using these assumptions, *Zolezzi and Seminara* [2001] obtained

$$\left(\varphi, v_0(\zeta), \frac{v_0(\zeta_0)}{\mathcal{F}(\zeta_0)}\right) = \sum_{i=0}^{2} \omega_i(k_i, G_i(\zeta), k_{i+3}) \tag{17}$$

$$h_0 = F_0^2 U^2 n \sum_{i=0}^{2} \varpi_i \tag{18}$$

with

$$\omega_{0,1,2} = \frac{D}{\chi_0}\left(UC, \frac{D(UC)_{,s}}{\chi_0}, \frac{UCD_{,s}}{\chi_0}\right), \tag{19}$$

$$\varpi_{0,1,2} = \left[a^{(0)}C, \chi_0 a^{(1)}(DC)_{,s}, \chi_0 a^{(2)} CD_{,s}\right], \tag{20}$$

$$k_i = \langle G_i \rangle \qquad (i = 0, 1, 2), \tag{21}$$

$$k_i = G_{i-3,\zeta}(\zeta_0) \qquad (i = 3, 4, 5). \tag{22}$$

The coefficients $a^{(i)}$ and the functions $G_i(\zeta)$ depend on the vertical profiles $\Gamma(\zeta)$ and $\mathcal{F}(\zeta)$ through the solutions of three second-order ordinary differential equations (ODEs) (see *Zolezzi and Seminara* [2001] for details). As will be seen in section 5, various models proposed in the past differ according to the formulation adopted for $\Gamma(\zeta)$. In particular, *Zolezzi and Seminara* [2001] used the formulation of *Dean* [1974] that corresponds to assuming a modified logarithmic law for the vertical profile of the main flow (see Appendix A). A slightly simplified logarithmic form was assumed by *Smith and McLean* [1984] and *Nelson and Smith* [1989b, 1989a], while a power law profile was used in the model by *Odgaard* [1986]. A very different assumption is based on *Engelund*'s [1974] slip velocity method and adopts a uniform eddy viscosity profile, $\nu_T = \alpha UD$, in which $\Gamma = \alpha = 0.077$ is very close to the depth-averaged value of Dean's $\Gamma(\zeta)$ used by Zolezzi and Seminara. This choice was adopted by *Kikkawa et al.* [1976], *Johannesson and Parker* [1989a], and *Bridge* [1992] and allows a more straightforward analytical evaluation of the coefficient $a^{(i)}$ and the functions G_i (the results are reported in Appendix A). In the discussion in section 5 concerning the different linear models, attention will only focus on Engelund's and Dean's eddy viscosity profiles since the other adopted vertical distributions can be considered as intermediate cases.

3.4. A Nonlinear Solution

[28] We conclude the general mathematical description of river meandering morphodynamics by developing a quite general method of solution for the full nonlinear problem. In this way we obtain a refined solution that will be used to test the more simplified linear schemes discussed in the following sections. Our approach to the nonlinear problem generalizes and extends the formulation by *Imran et al.* [1999] that uses an iterative scheme based on a procedure proposed by *Smith and McLean* [1984].

[29] We begin by writing each morphodynamic variable as the sum of a basic flow and a deviation, i.e.,

$$(U, V, D, H) = (1, 0, 1, H_0) + (u_1, v_1, d_1, h_1). \tag{23}$$

The perturbations u_1 and h_1 of the main flow and the surface level are then decomposed into the sum of a term with a zero mean in the transverse direction and a nonvanishing term that is only a function of s, that is

$$u_1 = \hat{u}(s, n) + \check{u}(s), \tag{24a}$$

$$h_1 = \hat{h}(s, n) + \check{h}(s) \tag{24b}$$

with

$$\overline{\hat{u}} = \overline{\hat{h}} = 0 \tag{25a}$$

$$\overline{h_1} - \overline{d_1} = 0, \tag{25b}$$

where (25b) is a local form of the integral condition (14b) and the overbar indicates lateral averaging. Hence, with the aid of equations (23)–(24), the nonlinear system (9)–(12) can be solved in an iterative way according to the following scheme

$$\hat{h}_{,n}^{\nu+1} = -R_3^{\nu}, \tag{26}$$

$$\hat{u}_{,s}^{\nu+1} + a_1 \hat{u}^{\nu+1} + \hat{h}_{,s}^{\nu+1} = R_1^{\nu} - \overline{R}_1^{\nu} + a_2 F_0^2 \check{h}^{\nu} - a_2 d_1^{\nu}, \tag{27}$$

$$\check{h}_{,s}^{\nu+1} - 2F_1(a_1 - a_2)\check{h}^{\nu+1} = \frac{F_1}{F_0^2}\left[\overline{R}_1^{\nu} - a_1 R_4^{\nu} - \frac{\partial R_4^{\nu}}{\partial s}\right], \tag{28}$$

$$\check{u}^{\nu+1} + F_0^2 \check{h}^{\nu+1} = R_4^{\nu}, \tag{29}$$

$$v_1^{\nu+1} = R_2^{\nu} - (n+1)\left(\check{u} + \check{h}\right)_{,s}^{\nu+1} - \frac{\partial}{\partial s}\left(\int_{-1}^{n} \hat{u}^{\nu+1} + d_1^{\nu} - \check{h}^{\nu+1} dn'\right), \tag{30}$$

where ν indicates the generic step of the iteration. In the previous relationships, $F_1 = F_0^2(1 - F_0^2)^{-1}$, while a_1 and a_2 are given in equation (50), the term R_3 is the left-hand side of equation (10) without the term involving H, and the terms

R_1, R_2, and R_4 arise from the nonlinear components of the system (9)–(12) and read

$$R_1 = \chi_1(1+F_0 2) + a_1 u_1 + a_2 d_1 - \frac{\beta C_f U\sqrt{U^2+v_1 2}}{ND} - Cv_1 U - \frac{1}{ND}\frac{\partial}{\partial n}[UD\varphi] - 2CU\varphi - u_1\frac{\partial u_1}{\partial s} - \frac{v_1}{N}\frac{\partial u_1}{\partial n}, \tag{31}$$

$$R_2 = -v_1(d_1 + nCD) - \frac{\partial}{\partial s}\int_{-1}^{n} d_1(u_1)dn'', \tag{32}$$

$$R_4 = -\breve{u}F_0^2\breve{h} - \overline{\tilde{u}\tilde{d}_1}. \tag{33}$$

[30] In particular, equation (27) is obtained by subtracting the lateral average from (9), while equation (28) is derived by combining equation (27) with the integral condition (14a); finally, equation (29) follows from (14a), and equation (30) derives from the continuity equation (11).

[31] The integration of the Exner equation (12), with the aid of constitutive relationships (16) and boundary conditions (13) and (25b), provides the last element of the iterative procedure

$$F_0^2 h_1^{\nu+1} - d_1^{\nu+1} = \int_{-1}^{n} \Lambda^{\nu} - \overline{\Lambda^{\nu}}dn', \tag{34}$$

where

$$\Lambda = \frac{\beta t^{*2}}{a\tau_n 2 + b\tau_s 2}\left[\frac{\gamma\tau_n}{t^*} + \frac{1}{q}\int_{-1}^{n'} N\left(q_{s,s} + Cq_n\right)dn''\right], \tag{35}$$

$$a = \frac{\gamma^2 t_c^*}{\mu q_0} q_{,t_0^*}, \tag{36a}$$

$$b = \gamma^2 \frac{r}{\sqrt{t_0^*}}, \tag{36b}$$

$$\gamma = \frac{U_0^2}{\hat{\rho}\tilde{d}_s}. \tag{36c}$$

At the first step of the procedure, $\breve{u} = \breve{h} = 0$ and the other variables (i.e., $\hat{u}$, v_1, $\hat{h}$, and d_1) are obtained from the linear solution (this could prevent convergence in the conditions close to resonance). Afterward, at the generic (ν + 1)th step of the iteration, the variables ($\hat{h}$, $\hat{u}$, $\breve{h}$, $\breve{u}$, v_1, and d_1)$^{\nu+1}$ are calculated by solving in cascade equations (26)–(30) and (34).

[32] The above scheme differs from that of *Imran et al.* [1999] in several points. For example, no spatial variability of the friction factor was originally considered. More importantly, the formulation now includes the full bed evolution, while *Imran et al.* [1999] only accounted for the fluid dynamic equations but not for the bed load transport equation (34), thus describing a nonlinear open channel flow on a fixed bed. Moreover, because of their more simplified lateral momentum equation (namely, the Euler equation) the R_3 term neither included the convection terms of the lateral flow nor the secondary currents driven by the bed stresses. This is equivalent to setting φ to zero, thereby eliminating the redistribution terms contained in R_1 from the main momentum equation (27). Although a linear term proportional to the curvature, i.e., $-A_s nC$, can be added to correct this limitation (see section 4.2), the lack of secondary currents prevents the modeling of the lateral bed stresses and consequently of the sediment transport dynamics. Apart from the term φ in R_1 the secondary currents v_0 also appear in the computation of the bed stresses t^*_i for the sediment equation and in the term φ_1 for the lateral momentum equation through the closure relationships (15)–(20). These relationships cause a feedback between the main flow and the secondary current, determining the nonlinear form of the model (26)–(30) and (34) [*Blanckaert and De Vriend*, 2004].

4. HIERARCHY OF LINEAR MODELS

[33] The linearization of the morphodynamic problem can be performed through the following perturbative expansions in the parameter ν_0 [*Parker*, 1976; *Ikeda et al.*, 1981; *Blondeaux and Seminara*, 1985; *Johannesson and Parker*, 1989a]

$$(U, V, D, H, C) = (1, 0, 1, H_0, 0) + \nu_0(u, v, d, h, \mathcal{C}), \tag{37}$$

$$\tau_s = C_{f0}\{1 + \nu_0(f_1 u + f_2 d)\}, \tag{38}$$

$$\tau_n = \nu_0 C_{f0}\left\{v + \frac{v_0(\zeta_0)}{\mathcal{F}(\zeta_0)}\right\}, \tag{39}$$

$$q = q_0\{1 + \nu_0(P_1 u + P_2 d)\}, \tag{40}$$

where the coefficients f_1, f_2, P_1, and P_2 that arise from the Taylor expansions of the functionals $C_f = C_f(t^*, D)$ and $q = q(t^*, D)$, which account for the spatial variation, read [*Parker*, 1976; *Blondeaux and Seminara*, 1985]

$$f_1 = \frac{2C_{f0}}{C_{f0} - t_0^* C_{f,t^*}|_0}, \tag{41a}$$

$$f_2 = \frac{C_{f,D}|_0}{C_{f0} - t_0^* C_{f,t^*}|_0}, \tag{41b}$$

$$P_1 = f_1\frac{t_0^* q_{,t^*}|_0}{q_0}, \tag{42a}$$

$$P_2 = f_2\frac{t_0^* q_{,t^*}|_0}{q_0} + \frac{q_{,D}|_0}{q_0}. \tag{42b}$$

[34] In the linear theory the terms v_0 and h_0 in (17) and (18) are simply modeled according to

$$v_0 = \nu_0\left(\chi_0^{-1} G_0 \mathcal{C} + \chi_0^{-2} G_1 \mathcal{C}_{,s}\right) \tag{43}$$

$$h_0 = \nu_0\left(F_0^2 a^{(0)} \mathcal{C} n + \chi_0 F_0^2 a^{(1)} \mathcal{C}_{,s} n\right). \tag{44}$$

[35] As a result the third addendum of the summations in equations (17) and (18) becomes redundant. The first terms of the right-hand side of equations (43) and (44) show a strong dependence on the curvature, while the second terms give rise to the phase lag of the secondary currents with respect to the curvature.

4.1. Three Key Linear Models: ZS_4, JP_2, IPS

[36] We can now describe the hierarchy of the linear models organically. As mentioned in section 1 we refer to three key linear models of river meandering morphodynamics. Our description starts from the most complete linear model proposed in the literature and then proceeds with more simplified ones.

[37] The most refined model (ZS_4) was proposed by *Zolezzi and Seminara* [2001]. They used *Dean*'s [1974] profile for the eddy viscosity and considered the spatial variation of the friction factor and sediment transport. Introducing the expansions (37)–(40) in (9)–(14), with the aid of (43), and neglecting the terms greater than $O(\nu_0)$, *Zolezzi and Seminara* [2001] obtained the following linear system

$$u_{,s} + a_1 u + h_{,s} + a_2 d = n b_1 \mathcal{C}, \tag{45}$$

$$v_{,s} + a_3 v + h_{,n} = b_2 \mathcal{C} + b_3 \mathcal{C}_{,s} + b_5 \mathcal{C}_{,ss}, \tag{46}$$

$$u_{,s} + d_{,s} + v_{,n} = 0, \tag{47}$$

$$a_4 u_{,s} + a_5 d_{,s} + v_{,n} + a_6\left(d - F_0^2 h\right)_{,nn} = 0, \tag{48}$$

with boundary conditions

$$\left(F_0^2 h - d\right)_{,n} = b_4 \mathcal{C} + b_6 \mathcal{C}_{,s}, \tag{49a}$$

$$v = 0 \qquad (n = \pm 1), \tag{49b}$$

and where the coefficients read

$$a_1 = f_1 \chi_1 \quad a_2 = \chi_1 (f_2 - 1), \quad a_3 = \chi_1, \tag{50}$$

$$a_4 = P_1, \quad a_5 = P_2, \quad a_6 = \frac{r}{\beta\sqrt{t^*}}, \tag{51}$$

$$b_1 = -\chi_1, \quad b_2 = 1 - \sqrt{C_{f0}} k_3, \quad b_3 = -\chi_0 k_0 - \frac{k_4}{\beta}, \tag{52}$$

$$b_4 = \frac{k_3\sqrt{t^*}}{r\sqrt{C_{f0}}}, \quad b_5 = -\chi_0^2 k_1, \quad b_6 = \frac{k_4\sqrt{t^*}}{\chi_1 r}. \tag{53}$$

Zolezzi and Seminara [2001] solved the linear system (45)–(48) using a Fourier expansion in the transversal direction, n, and obtained a fourth-order ODE for every Fourier mode. In particular, the equation for the streamwise velocity, $u = \sum_{m=0}^{\infty} u_m \sin(Mn)$ (with $M = \frac{1}{2}(2m+1)\pi$), gives

$$\frac{d^4 u_m}{ds^4} + \sigma_3 \frac{d^3 u_m}{ds^3} + \sigma_2 \frac{d^2 u_m}{ds^2} + \sigma_1 \frac{du_m}{ds} + \sigma_0 u_m = A_m \sum_{j=0}^{6} \rho_{j+1} \frac{d^j \mathcal{C}}{ds^j}, \tag{54}$$

where u_m is the mth Fourier mode and $A_m = 8(-1)^m[(2m+1)\pi]^{-2}$. The coefficients σ_{0-3} and ρ_{1-7} were given by *Zolezzi and Seminara* [2001] and in a simpler form are also reported in Appendix B. The model by *Zolezzi and Seminara* [2001] is indicated as ZS_4 to refer to the order of the differential equation (53) of the model.

[38] The solution of the linear differential equation (53) for all the modes allows one to obtain the value of the velocity at the bank, $u_b(s) = u(s, n = 1)$, which is necessary to simulate the meander evolution. The solution makes it evident that the flow field, and therefore also the river planimetry evolution, is regulated by (1) a local effect, (2) an upstream propagating influence, (3) a downstream propagating influence, (4) an upstream effect of the downstream boundary condition, and (5) a downstream effect of the upstream boundary condition [see *Zolezzi and Seminara*, 2001, equation (6.6)]. Therefore an upstream influence always occurs, both in subresonant ($\beta < \beta_R$) and superresonant ($\beta > \beta_R$) conditions, although it is only predominant in superresonant conditions.

[39] It can be shown that, because of linearization, the contribution of secondary currents only remains in the lateral momentum equation and in the sediment equation, so it only directly influences h and d. The linearization also makes the effect of the metric factor in equation (10) irrelevant, which justifies setting $N = 1$ in the computation of the secondary currents [e.g., *Odgaard*, 1986].

[40] A second family of models, called JP after *Johannesson and Parker* [1989a] [see also *Struiksma et al.*, 1985; *Crosato*, 1989], is obtained by assuming (1) a uniform vertical eddy-viscosity profile ($\Gamma = \alpha$; see Appendix A), (2) the friction coefficient, C_f, independent of D and $\mathbf{t}^*$, and (3) the bed load transport independent of depth, D. Using these assumptions, at the linear level one obtains $f_1 = 2$, $f_2 = P_2 = 0$, $P_1 = \frac{2f_0}{q_0} q_{,t^*}|_0$, whereas G_0 and $a^{(0)}$ are reported in Appendix A. Assuming $h^* = h_0 = \nu_0 F_0^2 a^{(0)} \mathcal{C} n$ [e.g., *Smith and McLean*, 1984; *Odgaard and Bergs*, 1988; *Nelson and Smith*, 1989b; *Bridge*, 1992], the linear system is reduced to three equations where the transverse component of the flow is no longer coupled with the dynamics of u and d. The coefficients in the linear system become

$$a_1 = 2\chi_1, \quad a_2 = -\chi_1, \quad a_3 = \chi_1, \tag{55}$$

$$a_4 = P_1, \quad a_5 = 0, \quad a_6 = \frac{r}{\beta\sqrt{t_0^*}}, \tag{56}$$

with $k_1 = k_4 = 0$ in (52) and (53). It follows that the m-Fourier mode of u is governed by the second-order equation

$$\frac{d^2u_m}{ds^2} + \sigma_1 \frac{du_m}{ds} + \sigma_0 u_m = A_m \sum_{j=0}^{3} \rho_{j+1} \frac{d^j \mathcal{C}}{ds^j}, \tag{57}$$

which, for $m = 0$, is formally equivalent to the model by *Johannesson and Parker* [1989a] (the coefficients $\sigma_{0,1}$ and ρ_{1-4} are reported in Appendix C). We refer to model (57) as JP_2 to recall the order of the differential equation. Note that *Johannesson and Parker* [1989b] also accounted for the phase lag due to the longitudinal convection of the lateral momentum between the secondary flow and the curvature and its derivative. For this purpose they used a modified curvature, $\sigma_s = \sigma_s(s)$, slightly shifted with respect to the curvature and driven by a first-order ODE, which is a semiempirical relaxation model derived from a simplified version of equation (46) (a similar approach is also given by *Struiksma et al.* [1985], *Olsen* [1987], and *Blanckaert and De Vriend* [2003]). However, as will be discussed in section 5, this effect can be reasonably neglected in natural rivers where such a lag is generally very small. Thus, unless otherwise specified, we will assume $\sigma_s \equiv \mathcal{C}$, which is equivalent to setting $\partial/\partial s = 0$ in (10). When the phase lag is considered instead, the corresponding model will be called JP_2^*.

[41] A last family of models, called IPS after *Ikeda et al.* [1981], can be obtained when, in addition to the hypotheses contained in the approach of the second-order models, the free response of bed sediment is neglected so that the bed topography has a constant lateral slope that is always in phase with the curvature. In other words, the sediment continuity equation is no longer coupled with the shallow water equations [e.g., *Engelund*, 1974; *Ikeda et al.*, 1981; *Kennedy et al.*, 1984; *Howard*, 1984; *Odgaard*, 1986; *Bridge*, 1992]. Such a simplifying hypothesis implies $q_n = 0$ throughout, so that the Exner equation reduces to $\eta_{,nn} = (F_0^2 h - d)_{,nn} = 0$, which means $(F_0^2 h - d)_{,n} = A$, where A is the constant slope factor. It follows that the resulting models include neither the resonance nor the upstream propagating influence.

[42] Furthermore, it is assumed that the only action of the secondary currents is to stabilize the lateral bed slope by means of topographic steering of the streamwise velocity, without any direct effect on the flow field. This means setting $\varphi = 0$ in (9) and reducing equation (10) to the Euler equation, which, after depth averaging and linearization, becomes $h^* = h_0 = \nu_0 F_0^2 \mathcal{C} n$. Formally, this result can be obtained by setting $a^{(0)} = 1$ and $a^{(1)} = 0$ in equation (44).

[43] With the previously mentioned hypotheses the linear system (45)–(49) reduces to

$$u_{,s} + a_1 u + a_2 d = n b_1 C - n\mathcal{C}_{,s} \tag{58}$$

$$d_{,n} = b_4 \mathcal{C} \tag{59}$$

with

$$d_{,nn} = 0 \quad (n = \pm 0) \tag{60a}$$

$$v = 0 \quad (n = \pm 1) \tag{60b}$$

and where

$$b_1 = -\chi_1, \tag{61a}$$

$$b_4 = F_0^2 - \frac{\sqrt{t_0^*} k_3}{r\sqrt{C_{f0}}}. \tag{61b}$$

As a result the following first-order differential equation is obtained

$$\frac{du}{ds} + a_1 u = (b_1 - a_2 b_4)\mathcal{C} - \frac{d\mathcal{C}}{ds}. \tag{62}$$

[44] In particular, the original model by *Ikeda et al.* [1981] corresponds to solving equation (62) at $n = \pm 1$, assuming (1) $N = 1$, and thus $b_1 = 0$, in the streamwise momentum equation, (2) a universal slope factor, and (3) no spatial variation of the friction factor, C_f, so that $a_1 = 2\chi_1$ and $a_2 = -\chi_1$. The second term of the parameter b_4 in (61b) is the slope factor defined by *Ikeda et al.* [1981] as A. In spite of its simplifications this model captures some fundamental features of meandering dynamics, such as fattening and skewing in meander evolution. This fact, together with its simplicity, explains its use in several theoretical and numerical works [e.g., *Parker et al.*, 1983; *Beck et al.*, 1984; *Parker and Andrews*, 1986; *Sun et al.*, 1996].

[45] The simple form of equation (62) allows a clear interpretation of the basic processes of meandering dynamics. The coefficient b_1 in the forcing term of the right-hand side accounts for the reduction in longitudinal convection associated with the outward decreasing of the longitudinal bed slope, while the coefficient b_4 of equation (62) derives from two responses to the centrifugally induced currents: the slope of the bed topography and the opposite slope of the free surface. These terms give two positive contributions to the outward shifting of the core of the downstream velocity, the former being stronger in alluvial rivers. The remaining forcing term is the effect of the vortex-induced stresses. In the left-hand side of equation (62) the free response of the streamwise velocity only depends on the coefficient χ_1, while the s derivative in the first term gives rise to the phase lag between u and the curvature in the presence of long stream changes in the planimetry, causing skewness in the bend evolution as well as the downstream propagating influence (such an influence has a characteristic spatial scale proportional to χ_1).

[46] In closing this section we note that the model given by equations (26)–(30) and (34) can be considered the natural nonlinear extension of ZS_4, and therefore we name it

ZS_{4N}. Moreover, the basic assumptions of the JP approach yield G_i from (A5),

$$\frac{\partial}{\partial s} = 0 \quad \text{in} \quad R_3, \tag{63}$$

$$\frac{\partial C_f}{\partial t^*} = \frac{\partial C_f}{\partial D} = \frac{\partial q}{\partial D} = 0, \tag{64}$$

from which, with the additional conditions $V = 0$ in R_3, we obtain the nonlinear model JP_{2N}. Finally, the natural nonlinear extension of the IPS model, called here IPS_N, is identical to the original formulation by *Imran et al.* [1999].

4.2. Some Extensions of the Original Linear Models: ZS_2, JP_4, IPS_U, and IPS_V

[47] Suitable modifications and extensions of the original linear models are useful to analyze the effect of the different morphodynamic processes. We begin with a simplified version of the ZS_4 model that helps one to understand the role of the topography-induced component of the surface level, $\hat{h}$. The key point is the approximated expression of the perturbation of the water surface level, h_0 in equation (44), obtained from the iterative procedure for the evaluation of the secondary currents. In the fourth-order model, ZS_4, such an expression is not used in the linearization of the flow equation, and h is left as an unknown quantity in the linear system. It is possible, however, to use the approximate solutions (44) and to reduce the linear problem to a system of three equation in three unknowns

$$u_{,s} + a_1 u + a_2 d = n b_1 \mathcal{C} + n b_1^{(1)} \mathcal{C}_{,s} + n b_1^{(2)} \mathcal{C}_{,ss}, \tag{65}$$

$$v_{,s} + a_3 v = b_2 \mathcal{C} + b_3 \mathcal{C}_{,s} + b_5 \mathcal{C}_{,ss}, \tag{66}$$

$$(1 - a_4) u_{,s} + (1 - a_5) d_{,s} - a_6 d_{,nn} = 0, \tag{67}$$

with the boundary conditions

$$d_{,n} = b_4 \mathcal{C} + b_6 \mathcal{C}_{,s} \quad v = 0 \quad (n = \pm 1). \tag{68}$$

[48] The coefficients a_{1-6}, b_1, and b_5 are reported by *Zolezzi and Seminara* [2001], while the remaining ones read

$$b_1^{(1)} = -a^{(0)}, \quad b_1^{(2)} = -\frac{a^{(1)}}{\chi_0}, \quad b_2 = 1 - \sqrt{C_{f0}} k_3 - a^{(0)}, \tag{69}$$

$$b_3 = -\frac{k_0}{\chi_0} - \frac{k_4}{\beta} - \frac{a^{(1)}}{\chi_0}, \quad b_4 = F_0^2 a^{(0)} - \frac{\sqrt{t_0^*} k_3}{r \sqrt{C_{f0}}}, \tag{70}$$

$$b_6 = \frac{F_0^2 a^{(1)}}{\chi_1} - \frac{\sqrt{t_0^*} k_4}{r \chi_0}. \tag{71}$$

[49] At this level of simplification the transversal component of the flow (66) is no longer coupled to the dynamics of u and d. It follows that the m-Fourier mode of u is governed by a second-order equation in a way that is formally similar to the JP_2 model (i.e., equation (57)). The respective coefficients σ_{0-1} and ρ_{1-4} are reported in Appendix C. This version, which will be referred to as ZS_2, lacks the full coupling between curvature-driven secondary currents (v_0) and the topography-driven lateral flow (V). Adopting equation (44) as the solution of the water level perturbation in fact implies neglecting the *super-elevation* of the water surface induced by the topography and thus its effect on the transversal flow. In this way, v_0 influences V, but the opposite is no longer true. To test this point, a numerical comparison between ZS_4 and ZS_2 will be shown in section 5.

[50] Alternatively, we may extend the original JP_2 model to a fourth-order version by avoiding the assumption $h^* = h_0 = \nu_0 F_0^2 a^{(0)} \mathcal{C} n$ (see Appendix B for the coefficients). This generalized version of the JP_2 model, called JP_4, is mathematically similar to ZS_4 and includes an upstream propagating influence in subresonant conditions but has quantitative differences in both the free and forced response of the system (see section 5).

[51] It is important to note that *Johannesson and Parker* [1989a] introduced a correction term, A_s, to account for the fact that, upon linearization, the second-order model JP_2 loses any influence of the dispersive term φ in (9); in the linear context the solution of the secondary currents (43) and the vertical profile of longitudinal velocity $\mathcal{F}$ do not, in fact, depend on n. To overcome this fact, they extended the solution of the flow field, only valid in the central part of the stream, to the sidewall boundary layers, thus forcing the longitudinal velocity to drop to zero at the wall. As a result they could account for the bank effect on the redistribution term, which becomes of the order of $O(\nu_0)$, and they added a correction term, A_s, that is similar to the slope factor A. The results resolved the contradiction between the linear theory and the data by *Kikkawa et al.* [1976] for a vanishing bed slope [*Johannesson and Parker*, 1989c] besides allowing $v = 0$ to be set at the wall and not at the edge of the boundary layer as in 2-D models. However, the approximation used is rather crude, since the velocity profile in the boundary layer is assumed to have the same behavior as in the central part. Consequently, a sharp discontinuity appears at the wall and the "momentum method" leads to a dispersive term that is a Dirac delta function placed at the wall, resulting in an overestimation of A_s for narrow rivers. In the present work, in order to compare the fourth- and second-order models coherently, we will set $A_s = 0$ and simply use JP_2 (as done by *Parker and Johannesson* [1989] when comparing their model with that of *Blondeaux and Seminara* [1985]).

[52] Finally, some extensions of the original IPS formulation are naturally suggested by the generalization of the slope factor term A in equation (62). *Ikeda et al.* [1981] assumed a slope factor that is independent of the local hydraulic characteristic [see also *Kikkawa et al.*, 1976;

TABLE 1. Main Characteristics of the Mentioned Models

Model	Characteristics
ZS_4	vertically varying eddy viscosity [$\Gamma = \Gamma(\zeta)$] full coupling between the longitudinal and the transverse flow momentum full coupling between the fluid and sediment dynamics spatial dependence of the friction factor on D and t^*
ZS_2	as ZS_4 except for the coupling in the flow momentum
JP_4	uniform eddy viscosity ($\Gamma = \alpha$) full coupling between the longitudinal and the transverse flow momentum no spatial dependence of the friction factor on D and t^*
JP_2^*	as JP_4 except for the coupling in the flow momentum
JP_2	as JP_2^* but no phase lag of the secondary current
IPS_U	as JP_2 but no coupling with the sediment dynamics
IPS_V	as IPS_U but the bed slope factor comes from a slowly varying eddy viscosity approach

Zimmermann and Kennedy, 1978]. A constant value was also assumed by other researchers [e.g., *Beck et al.*, 1984; *Sun et al.*, 1996]. However, it seems to be more realistic to evaluate the slope factor considering the effect of secondary currents on the bed by means of the value k_3, since by the equations (13) and (16) it is straightforward to show that $A = -(k_3/r)\sqrt{t_0^*/C_{f0}}$. Thus, as the structure of the secondary currents depends on the eddy viscosity model (through $k_3 = G_{0,\zeta}(\zeta_0)$), we will consider both the solution with a uniform value of ν_T and the solution with a variable value for ν_T, obtaining two extensions of the IPS model, called IPS_U and IPS_V, respectively.

5. ANALYSIS OF THE LINEAR MODELS

[53] In the following the free response and the structure of the forcing term are analyzed for each linear differential model described in section 4 (Table 1 summarizes their characteristics). The free response defines the self-excited response of the system, the resonant condition, and the upstream and downstream influence on the local lateral erosion. Instead, the forcing term contains the information about the planimetric curvature, gives the local influence on the erosion, and provides a particular solution of the system.

5.1. Free Response: Eigenvalues, Resonance Conditions

[54] For realistic values of the morphodynamic parameters, the fourth-order models (ZS_4 and JP_4) almost always have two real wave numbers, λ_1 and λ_2, and two complex-conjugate wave numbers, λ_3 and λ_4, while only a small range of β exists with four real solutions [*Struiksma et al.*, 1985; *Seminara and Tubino*, 1992]. The second-order models (ZS_2 and JP_2) have two solutions, either complex-conjugate or real, whereas IPS models have only one characteristic wave number equal to $-2\chi_1$. Since a recursive relation among the eigenvalues exists for each model, e.g., $\lambda_i^{(m)}(\beta) = m\lambda_i^{(1)}(\beta/m)$ for ZS_4 [*Seminara and Tubino*, 1992], we have only studied the first two modes ($m = 0, 1$).

[55] Figure 4a shows the influence of the aspect ratio on the eigenvalues of the fourth-order models ($t_0^* = 0.1$, $d_s = 0.01$, $m = 0$, and flat bed conditions). The JP_4 model has a qualitatively similar behavior to ZS_4. Quantitatively speaking, however, the two theories only agree for either very small or very large values of β (greater than 100), but this is generally outside the range of validity of the shallow water theory (small β) or in the braiding regime (large β, though huge meandering rivers can have very large values of β). Such discrepancies underline the importance of the expansion of the friction factor made in the ZS approach, which is the only difference in the free response between the two models. On the other hand, such an expansion does not affect the qualitative behavior of the system response, since both models can have superresonant conditions and always present an upstream propagating influence (i.e., λ_1 is always positive). We have verified these findings for a wide range of t_0^* and d_s as well as for the case of dune-covered beds. Similar considerations can be drawn from the comparison between the eigenvalues of the ZS_2 and JP_2 models plotted in Figure 4b. By comparing Figures 4a and 4b it can also be pointed out that the eigenvalues of the second-order models have behavior that is very close to that of λ_3 and λ_4 in the fourth-order models.

[56] The behavior of $\lambda_{IPS} = -2\chi_1$ is represented by the decreasing straight line in Figures 4a and 4b. Despite the fact that the IPS model cannot reproduce the full gamut of processes described in section 2, in some cases it can give a rough estimate of the predominant wave number. Figure 4a, in fact, shows that a range exists in which λ_{IPS} is comparable to the smaller eigenvalues of the fourth-order models; that is, $\lambda_{IPS} = O[\mathrm{Re}(\lambda_3), \mathrm{Re}(\lambda_4)]$. As such eigenvalues dictate the scale of the morphodynamic memory, this implies that the first-order models are able to capture the essential spatial scale of meandering dynamics. Outside this range of β they are too simplified and can only give a coarse description of the process. Moreover, apart from the near-resonant conditions where all the linear models fail, the IPS models cannot describe the superresonant case. It can be shown, however, that the range of validity of IPS increases for higher modes.

[57] We close this section by discussing the resonance condition that takes place when $\beta = \beta_R$, i.e., when the real part of the complex eigenvalues is zero. In both ZS_4 and

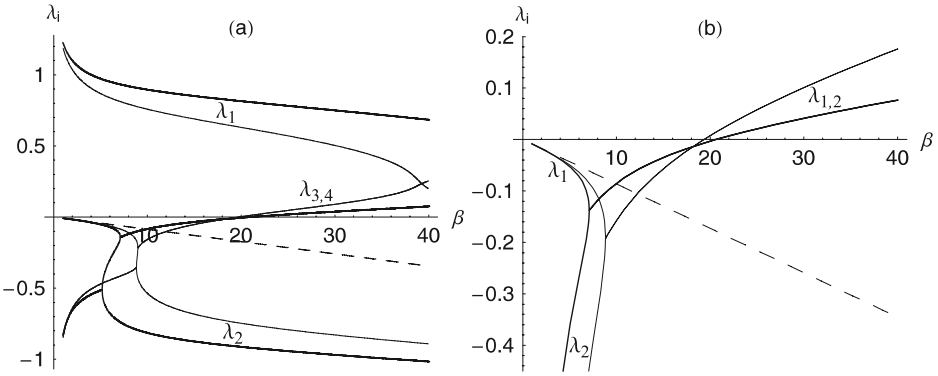

Figure 4. Behavior of the real part of the eigenvalues in the case of (a) fourth-order and (b) second-order models ($m = 0$, $t_0^* = 0.1$, $d_s = 0.01$, and flat bed). ZS_4 and ZS_2 are indicated by bold lines; JP_4 and JP_2 are indicated by thin lines. The dashed line corresponds to the *Ikeda et al.* [1981] approach.

ZS_2 the resonant condition is met when the two complex eigenvalues have a vanishing real part. For ZS_2 the computation of the resonant aspect ratio, β_R, can be readily computed from the condition $\sigma_1 = 0$, since the term involving σ_1 plays the role of a resistive term in a forced damped oscillator, which becomes resonant when the resistance vanishes. In this way one obtains [see also *Parker and Johannesson*, 1989]

$$\beta_R = M\sqrt{\frac{r}{C_{f0}\sqrt{t_0^*}[(f_2-1)(1-P_1)+f_1(P_2-1)]}}, \qquad (72)$$

and in the same way one may obtain the respective simplified formula for the JP scheme.

[58] Figures 5a and 5b compare the values of β_R for the fourth- and second-order models as a function of the Shields stress. The good accuracy provided by the second-order models, which improves for low d_s, is evident and suggests that equation (72) can be useful to easily verify whether a river is in subresonant or superresonant conditions. On the other hand, the difference between the JP and ZS approaches confirms the important role of the spatial variation of the friction factor due to the local hydrodynamic conditions.

5.2. Forcing Term: Secondary Currents

[59] The nonhomogenous part of the linear models represents the forcing term because of the influence of the planimetric curvature on the secondary currents. We discuss here the dispersive term φ and the transversal bed stress τ_n that account for the effects of secondary currents on the formation of the near-bank excess velocity. We begin with the most complete model, i.e., ZS_4, in which these quantities have the structure

$$\varphi = \nu_0 k_0 \frac{\mathcal{C}}{\chi_0} + \nu_0 k_1 \frac{\mathcal{C}_{,s}}{\chi_0^2} \qquad (73)$$

$$\tau_n = \nu_0 C_{f0} v + \nu_0 C_{f0}\left[k_3 \frac{\mathcal{C}}{\chi_0} + k_4 \frac{\mathcal{C}_{,s}}{\chi_0^2}\right]. \qquad (74)$$

[60] In these equations, k_0 and k_3 give the in-phase contribution of the secondary currents, derived from the first term of the right-hand side of (73) and (74), whereas k_1 and k_4 provide the phase lag contribution of the secondary currents, derived from the second term in the right-hand side of (73) and (74). Such a phase lag was pointed out by *Yen* [1972] and *Gottlieb* [1976] and modeled by *Zimmermann and Kennedy* [1978]; *Kitanidis and Kennedy* [1984]; *Struiksma et al.* [1985]; *Ikeda and Nishimura* [1986]; *Johannesson and Parker* [1989b], and *Zhou et al.* [1993]. However, these authors also noticed that the phase lag in alluvial rivers is always much smaller than that observed in laboratory experiments (see also the observations by *Odgaard and Kennedy* [1982]), because of both the smaller depth-arc-length ratio and the greater friction factor [*Zhou et al.*, 1993]. This is confirmed by an order-of-magnitude analysis of (73) and (74). In natural rivers, χ_0 is usually of the order of 10^0–10^1, whereas $\mathcal{C}$ varies in the range [10^{-2}–10^0] and $\mathcal{C}_{,s}$ is at most of the order of $\mathcal{C}^3$ [e.g., *Parker and Andrews*, 1986]. Thus, since the coefficients k_0 and k_3 are of the same order of magnitude as k_1 and k_4, the phase-lagged contribution to both dispersive and lateral bed stress is usually 3 or 4 orders of magnitude less than that of the in-phase part. As a result the forcing term can be discussed focusing only on the coefficients k_0 and k_3.

[61] In the linear system (45)–(48) the dispersive term, φ, acts only in the lateral momentum equation through the coefficients b_3 and b_5. We have shown that in the second-order models such an equation becomes decoupled from the other ones; thus the dispersive term neither influences the streamwise momentum nor the erosion process. This means that neglecting the effect of the topography-driven lateral flow on the secondary currents, as in (65) and (67), is equivalent to neglecting the dispersion process. In contrast, in fourth-order models (ZS_4 and JP_4) the lateral momentum is coupled with the streamwise momentum, and hence the lateral dispersion of momentum is important. Figure 6a shows the behavior of k_0 for ZS_4 and JP_4. It can be seen that this term is always more important in the former model. Moreover, only for the JP_4 model, the influence of k_0 becomes negligible when d_s is small.

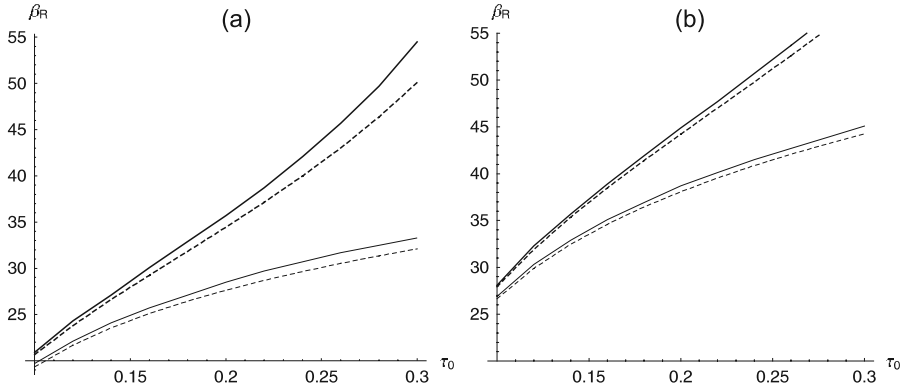

Figure 5. Behavior of β_R versus t_0^* for (a) $d_s = 0.01$ and (b) $d_s = 0.001$. The bold lines refer to the ZS approach, while the thin lines refer to the JP approach (fourth-order models (solid lines) and second-order models (dotted lines)).

[62] Figure 6b shows the coefficient k_3 that describes the effect of the secondary current on the lateral bed stresses. Such a process is present in all the models that have been analyzed and can be considered as one of the main driving factors of meandering. We can see that the JP approach underestimates the effect of the secondary currents, compared to the ZS approach. This main difference in the forcing term is mostly due to the different modeling of the eddy viscosity, which yields two different vertical distributions for both the main flow and the secondary currents, as shown in Figures 7a and 7b (see also Appendix A). In particular, the uniform eddy viscosity approach (thin lines) underestimates the bed stresses. In conclusion, since the phase lag of the secondary currents and the role of the dispersive term are usually negligible, the actual impact of the secondary current on meandering dynamics is very sensitive to the turbulence-closure model that is employed. This fact also justifies the introduction of the improved IPS models, i.e., IPS_U and IPS_V.

6. EXPERIMENTAL VERIFICATION OF THE LONGITUDINAL FLOW FIELD

[63] We tested the performance of the linear models and verified the use of *Kalkwijk and De Vriend* [1980] decomposition (8) in the nonlinear approach using two sets of experimental data obtained by *Whiting and Dietrich* [1993a, 1993b] in a bend flow. The considered experiments report the downstream surface velocity in two symmetric sine-generated channels of a 25 cm wide flume, with a nonerodible flat bed and an erodible bed, called run 100-5 and run 115-3, respectively, by Whiting and Dietrich. By assuming a lateral boundary layer width equal to the half depth, the morphodynamic parameters are equal to $\beta = 5.75$, $t_0^* = 0.076$, and $d_s = 0.031$ for run 100-5 and $\beta = 7.3$, $t_0^* = 0.045$, and $d_s = 0.038$ for run 115-3. As a consequence, the shallow water hypothesis (i.e., $\beta > 5$) is satisfied. Figure 8 shows a comparison between the experimental measurements, the linear model ZS_4, and the proposed nonlinear approach, in which the solution of ZS_4 has been used as the first step of the iterative procedure. In the simulations the surface velocity is obtained from the depth-averaged velocity using the vertical profile derived from *Dean*'s [1974] assumptions on eddy viscosity.

[64] The left side of Figure 8 shows the hydrodynamic computation with a flat bed (run 100-5) and suggests that the linear model, although giving a very smooth pattern, is able to capture the correct range of surface velocities (15–25 cm/s), with the maximum velocity at the inner bank. In such a case the topographic steering driven by the lateral

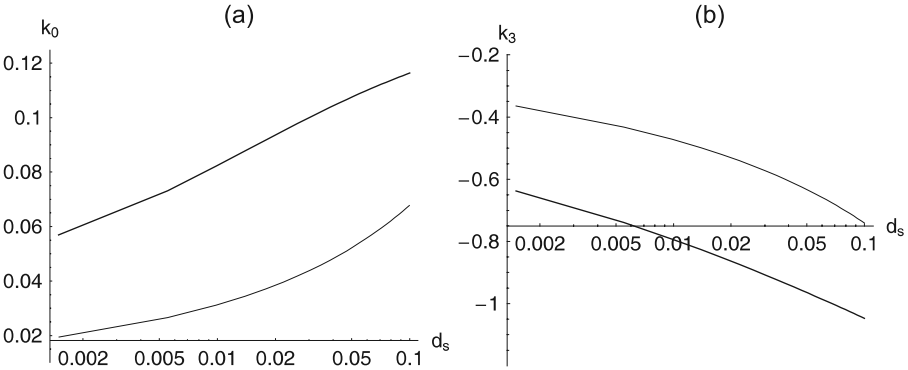

Figure 6. Dependence of (a) k_0 and (b) k_3 on d_s. ZS_4 and ZS_2 are indicated by bold lines; JP_4 and JP_2 are indicated by thin lines.

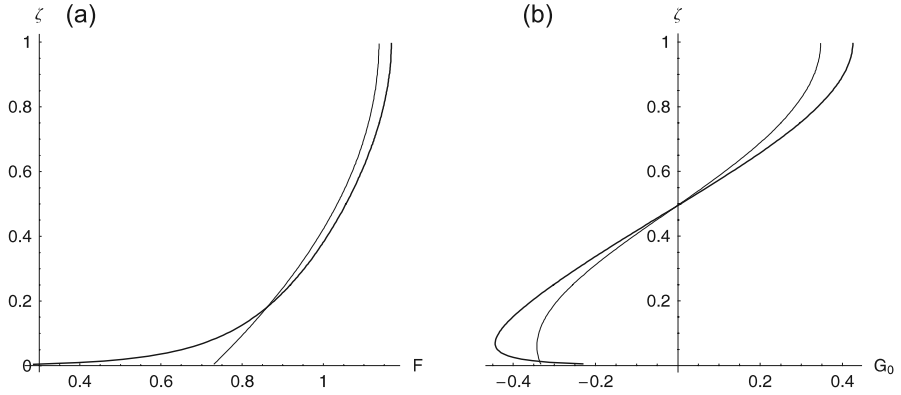

Figure 7. Vertical profiles of the (a) main flow ($\mathcal{F}$) and (b) secondary currents (G_0) for the ZS approach (bold lines) and the JP approach (thin lines) in the case of a flat bed.

slope bed is absent, so the superelevation of the free surface induces an increase in the velocity where the pressure is low, i.e., at the inner bank. On the other hand, the nonlinear model improves the picture by moving the peak velocity toward the center of the channel and giving "a corridor of high velocity which crosses from the convex to the concave bank," as was experimentally observed by *Whiting and Dietrich* [1993b, p. 3620].

[65] The comparison with the erodible bed experiment (run 115-3), reported on the right side of Figure 8, shows how the linear model predicts the main features of the flow field, with the correct values of the maximum velocity at the out bank and with a substantially correct phase lag with respect to the curvature. Because of the influence of the nonlinear sediment equation (34) the nonlinear model works even better than in the flat bed case. The model reproduces the main spatial heterogeneities of the surface flow field and, in particular, the high-velocity island before the apex bend followed by a large zone with a relatively low velocity. However, the isolated high-velocity region after the bend apex (Figure 8b) is not predicted.

[66] In conclusion, both the linear and the nonlinear models are able to predict the right value of the longitudinal velocity at the outer bank. As a consequence they can be reasonably adopted for the computation planimetric evolution of the river (see hypothesis 4 in section 3.1). However, it should be noticed that the whole planimetric distribution of the flow field reported in the previous experiments is not reproduced exactly. This is expected in a 2-D approach, particularly in the case of a low aspect ratio. For this reason the models work better if applied to the conditions of run 115-3 (β = 7.3) compared to run 100-5 (β = 5.75). Moreover, the unsteady "shingle bar unit" observed in the experiments by *Whiting and Dietrich* [1993a] cannot be obtained by any steady state morphodynamic theory.

7. PLANIMETRIC EVOLUTION

[67] In this section we assess the quantitative influence of the different morphodynamic processes by comparing the meander evolution produced by the previously described models.

7.1. Geometric Formalism

[68] The evolution of the river planimetry can be interpreted as the dynamics of a curve moving on a plane through elongations and lateral displacements. Consequently, the problem can be treated using the formalism of the differential geometry of one-dimensional curves. A similar approach is implicit in all the numerical simulations of meandering models [e.g., *Howard*, 1984; *Stølum*, 1996; *Sun et al.*, 1996, 2001a; *Seminara et al.*, 2001] and was used explicitly by *Seminara et al.* [1994]. Here we present a formal and general deduction of the integrodifferential equation regulating the geometric evolution of the curve [e.g., *Brower et al.*, 1984; *Nakayama et al.*, 1992].

[69] The equation of motion of a parameterized curve $\mathbf{r}(\alpha, t)$ that moves along the normal unit vector $\mathbf{n}$ (see Figure 3a) is

$$\frac{\partial}{\partial t}\mathbf{r}(\alpha,t) = \mathbf{n}\Upsilon\left[\mathbf{r}(\alpha,t), \frac{\partial \mathbf{r}(\alpha,t)}{\partial \alpha}, \ldots\right], \tag{75}$$

where Υ is a functional that represents the normal displacement rate and α is a purely descriptive parameter that is independent of time, so that $\frac{\partial}{\partial t}\frac{\partial}{\partial \alpha} = \frac{\partial}{\partial \alpha}\frac{\partial}{\partial t}$. Introducing the arc length coordinate $\tilde{s}(\alpha, t) = \int_0^\alpha \sqrt{\psi} d\alpha'$, where $\psi(\alpha, t) = |\frac{\partial \mathbf{r}}{\partial \alpha} \cdot \frac{\partial \mathbf{r}}{\partial \alpha}|$, we obtain (with $\tilde{C} = |\partial^2 \mathbf{r}/\partial \tilde{s}^2|$)

$$\frac{\partial}{\partial t}\frac{\partial}{\partial \tilde{s}} - \frac{\partial}{\partial \tilde{s}}\frac{\partial}{\partial t} = -\tilde{C}\Upsilon\frac{\partial}{\partial \tilde{s}}. \tag{76}$$

[70] Equation (76), along with the Serret-Frenet equation [*Do Carmo*, 1976], provides the temporal rate of change of the arc length coordinate

$$\begin{aligned}\frac{\partial \tilde{s}}{\partial t} &= \frac{\partial}{\partial t}\int_0^\alpha \sqrt{\psi} d\alpha' = \int_0^\alpha \frac{1}{2\sqrt{\psi}}\frac{\partial \psi}{\partial t} d\alpha' \\ &= \int_0^\alpha \frac{1}{2\sqrt{\psi}} 2\psi \tilde{C}\Upsilon d\alpha' = \int_0^{\tilde{s}} \tilde{C}\Upsilon d\tilde{s}',\end{aligned} \tag{77}$$

which permits equation (75) to be written in the integrodifferential form

$$\frac{\partial \mathbf{r}(\tilde{s},t)}{\partial t} = \mathbf{n}\Upsilon - \frac{\partial \mathbf{r}(\tilde{s},t)}{\partial \tilde{s}}\int_0^s \tilde{C}\Upsilon d\tilde{s}', \tag{78}$$

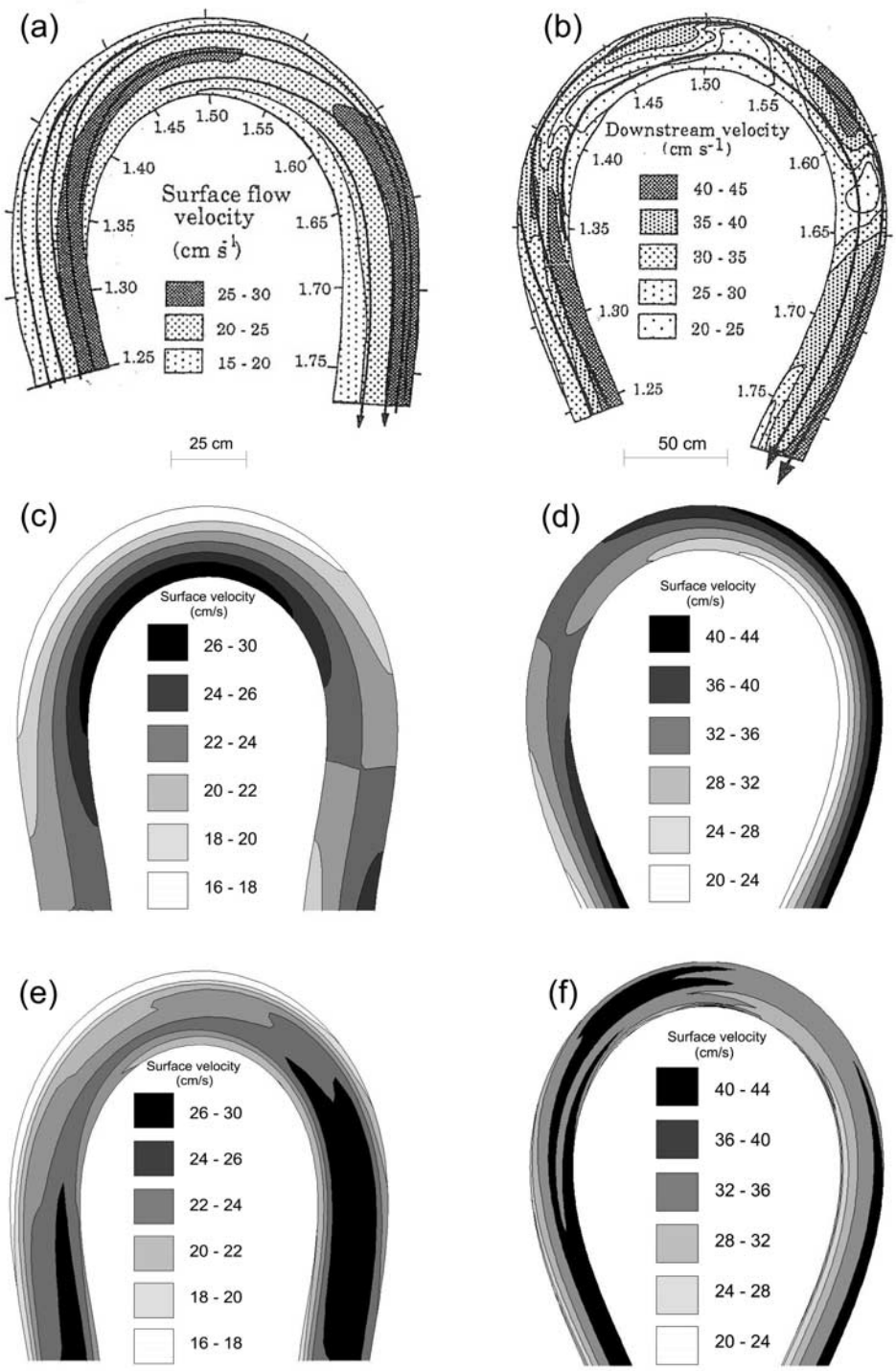

Figure 8. Comparison of the experiments by *Whiting and Dietrich* [1993a, 1993b], the linear model by *Zolezzi and Seminara* [2001], and the proposed nonlinear approach. (left) Run 100-5 ($\beta = 5.75$, $t_0^* = 0.076$, and $d_s = 0.031$). (right) Run 115-3 ($\beta = 7.3$, $t_0^* = 0.045$, and $d_s = 0.038$). (a and b) Laboratory data. (c and d) ZS linear theory. (e and f) Nonlinear model.

where the normal velocity Υ is the dynamic term that drives the curve evolution. Once the normal velocity Υ is known, the latter equation allows the evolution of the plane curve to be described. A scalar form of equation (78), deduced following a different approach, was also reported by *Seminara et al.* [1994, 2001].

[71] It is important to notice that equation (78) has a spatial memory term and is inherently nonlinear, independently of the "dynamic" nonlinearities introduced by Υ that depend on the meandering model adopted. As mentioned before, the normal velocity Υ is usually assumed to be proportional to the velocity excess at the bank, u_b, through an erodibility coefficient, E. Consequently, we can compare

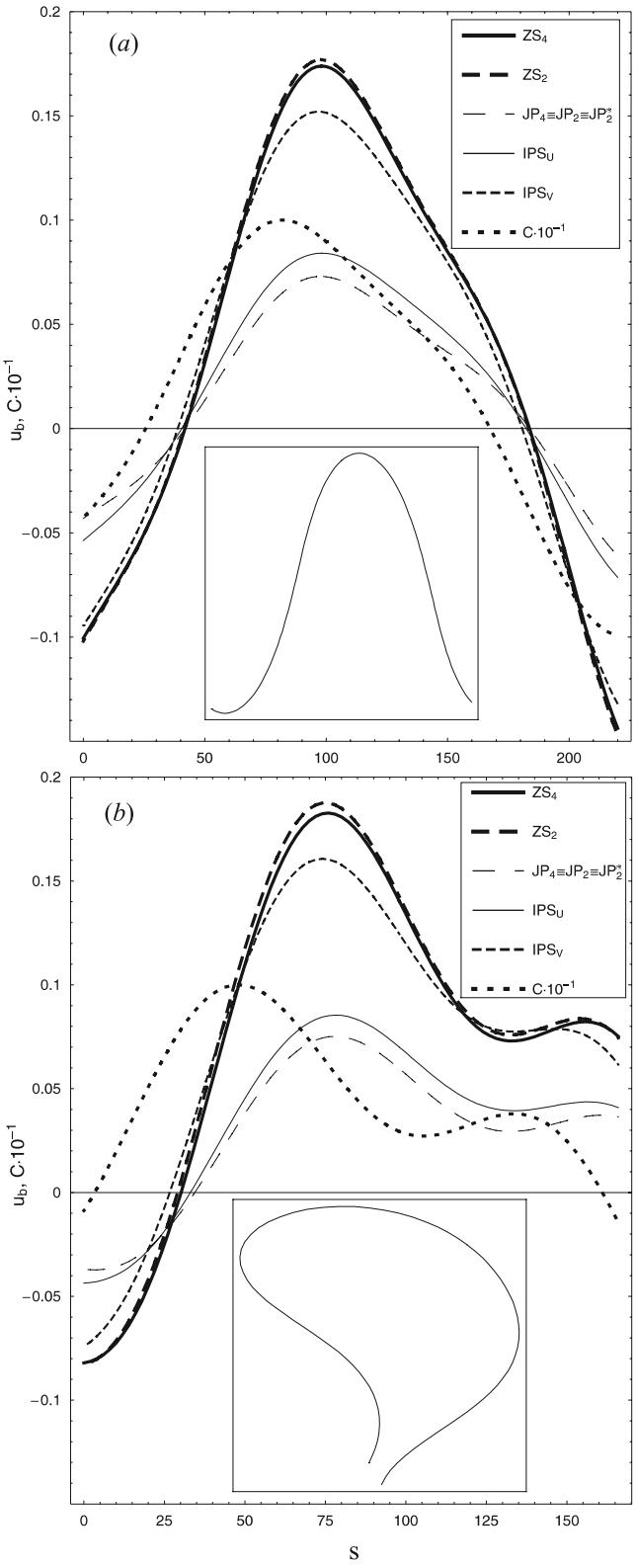

Figure 9. Behavior of u_b for the different models in the case of a Kinoshita-shaped meander with (a) $\theta_0 = \frac{\pi}{3}$, $\theta_1 = \pi^3/1184$, $\theta_2 = \pi^3/864$, and $k = 0.02$ and (b) $\theta_0 = \frac{2}{3}\pi$, $\theta_1 = \pi^3/648$, $\theta_2 = \pi^3/108$, and $k = 0.02$. The insertions show the shape of the meanders in the two cases.

the river evolutions described by the different meandering models by focusing directly on the differences between the dynamics of u_b.

7.2. Linear Regime

[72] We next compare the evolution of the original models, ZS_4, JP_2 (along with its variant JP^*_2), and IPS, as well as the extensions ZS_2, JP_4, IPS_U, and IPS_V (see Table 1). Figures 9a and 9b show the linear behavior of u_b for two sets of morphodynamic parameters, with $\beta = 13$, $t^*_0 = 0.32$, and $d_s = 0.003$. In both cases the *Kinoshita curve* [*Kinoshita*, 1961] is chosen as a typical meander planimetry. It describes the precutoff meander shape well [*Parker and Andrews*, 1986; *Seminara et al.*, 1994] by means of the equation

$$\theta = \theta_0 \sin(ks) + \theta_1 \sin(3ks) + \theta_2 \cos(3ks), \tag{79}$$

where θ is the angle with respect to the x coordinate (see Figure 3a) and $k = 2\pi/L_m$. Figure 9a refers to a medium large-amplitude meander, whereas Figure 9b refers to a configuration at incipient cutoff. The great difference in amplitude in the models, particularly the ZS models, is the most evident aspect, while the phase is nearly the same for all models. In particular, IPS_U and JP_2 are very close to each other, while JP^*_2 is practically coincident with JP_2, thus supporting the hypothesis of neglecting the phase lag of the secondary current in this model. The only difference between IPS_U and JP_2 models is that the former does not account for the free response of the sediment transport; the substantial agreement of their u_b behaviors confirms that the free response of the bed topography does not have any significant influence in mildly sinuous channels [see *Kinoshita*, 1961; *Tubino and Seminara*, 1990].

[73] The differences between second-order and fourth-order models are generally very small, with the former ones having slightly higher amplitudes, especially in the JP approach. The small differences result from the distribution term of the lateral momentum through the main flow transport (modeled only in the fourth-order models), which seems to have a little effect on the longitudinal velocity, thus supporting the interest for second-order models.

[74] Finally, the behavior of the IPS_V model is particularly interesting. In this model the slope factor implicitly follows from the use of *Dean*'s [1974] eddy viscosity profile, which gives a lateral bed stress response that is stronger than that of *Engelund*'s [1974] method. For this reason, IPS_V shows an amplitude response that is larger than the original IPS model and in good agreement with that of ZS_4. Once more, this underlines the strong sensitivity of the results to the modeling of secondary currents. Although in other morphodynamic conditions the agreement between ZS_4 and IPS_V may not be as good, IPS_V represents a good compromise between parsimony and detail (which could even be improved by accounting for the influence of the spatial variation of C_f).

[75] Although the differences in phase among the models are small, they are even more important than those in

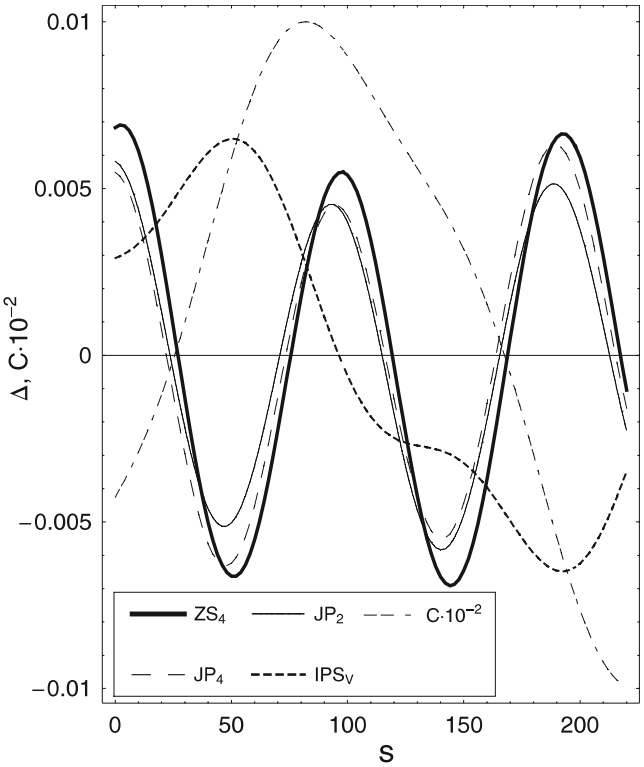

Figure 10. Behavior of $\Delta_i(s)$ along the Kinoshita-shaped meander with $\theta_0 = \pi/3$.

amplitude, as the latter can be absorbed in the uncertainties in the value of the erodibility coefficient E, which is usually evaluated by fitting the model results to real data. In order to compare the phase differences and the behavior of $u_b(s)$ for the various models we use ZS_4 as the reference model, evaluating for each model (i) the value of the coefficient δ_i that minimizes the difference $[\delta_i u_b^i(s) - u_b^{ZS_4}(s)]$. We then analyze the quantity $\Delta_i(s) = [\delta_i u_b^i(s) - \delta_{IPS_U} u_b^{IPS_U}(s)]$, in which the simplest model, IPS_U, is now used as a reference for the plotting. Such a procedure allows the smallest differences between the models to be amplified and analyzed. Figure 10 shows an application to the Kinoshita curve with $\theta = \pi/3$. Comparing the responses of the models, both differences and analogies are evident. The third harmonic present in the Kinoshita curve induces a high-frequency response in all the models. However, the high harmonic has a small amplitude in the first-order models (IPS_U and IPS_V), while it is more prominent in the higher-order models. The behavior of Δ_{IPS_V} suggests that improving the slope factor evaluation in the IPS approach changes both the amplitude and the phase, as previously argued by *Parker et al.* [1983]. The strong sensitivity of the higher-order models to the third harmonic of the planimetric forcing can be related to the complex conjugate eigenvalues that characterize the ZS and JP models. Complex eigenvalues, in fact, induce an oscillating solution which, in particular conditions, can be in a resonant (or near resonant) state with the forcing third harmonic rather than with the leading harmonic. This third-harmonic resonant state is dictated by $\beta = \beta_R$ and $\mathrm{Im}(\lambda_c) = 3k$, where λ_c is the complex conjugate eigenvalue. Such patterns can affect the frequency spectrum of the river planimetry, favoring the growth of the higher harmonics (i.e., multilobing). Despite the fact that, in general, the growth of higher-order harmonics is slow and that cutoff happens before they become noticeable, the river long-term evolution can be influenced by them in the form of characteristic multilobes in the river pattern. It is important to distinguish this multilobing, which has a fluid dynamic origin, from cutoff-induced multilobing, which has a "geometric" origin because of the impossibility of self-intersection in the river planimetry.

[76] The evolutions predicted by the different models have been compared, using both the same value of the erodibility coefficient, E, and the modified value, $\delta_i E$. Equation (78) is solved numerically by a step-to-step shifting and fitting. In particular, Figures 11a and 11b report the reaches after 3000 years starting from the same Kinoshita curve with $\theta_0 = \pi/3$ for ZS_4, JP_2, and IPS_U. Very similar behavior can be noticed for JP_2 and IPS_U, while ZS_4 provides a more skewed configuration as well as a more rapid evolution (Figure 11a).

[77] The reliability of the linear models has been investigated, in cases with nonnegligible curvature, by comparing the linear and nonlinear versions for each approach (*Seminara and Tubino* [1992] performed a weakly nonlinear analysis of the ZS approach but they referred to nearly resonant conditions). Figure 12 shows the comparison between the three linear models, ZS_4, JP_2, IPS_U, and the respective nonlinear extensions. We can notice that the phase is also preserved in the nonlinear models, underlining the importance of the real negative eigenvalue of the linearized problem even in the nonlinear models. Only IPS_{UN} shows a small lag compared to IPS_U in agreement with *Imran et al.* [1999], who noticed that the greatest discrepancies between the linear and nonlinear models are associated with large values of scour factor A (greater than 3). However, even though $A \simeq 10$ in the present case, this difference appears to be small compared to the difference between ZS_4 and IPS_U.

7.3. Comparison With a Field Case

[78] The evolutions predicted by the three original linear models (i.e., IPS_U, JP_2, and ZS_4) have been tested on a real case. Such an analysis allows us to test and compare models of different complexity on a real case with the aim of evaluating the role of the morphodynamic processes involved in meandering dynamics. Some works [*Beck et al.*, 1984; *Howard*, 1984] have already compared real and predicted river evolutions but used only the first-order model IPS_U.

[79] Here we focused on a 3.5 km reach of the Tanaro River, a tributary of the Po River, in northwest Italy. The mean annual discharge is 70 m^3/s, the mean sediment roughness is 2.3 mm, the mean depth is about 1.2 m, the bed slope is 0.0006, and the width is about 70 m. The planimetry of this reach in 1880 and 1991 was obtained from the Italian Geographic Military Institute (see Figure 13, where, for the sake of clarity, only the river axes are

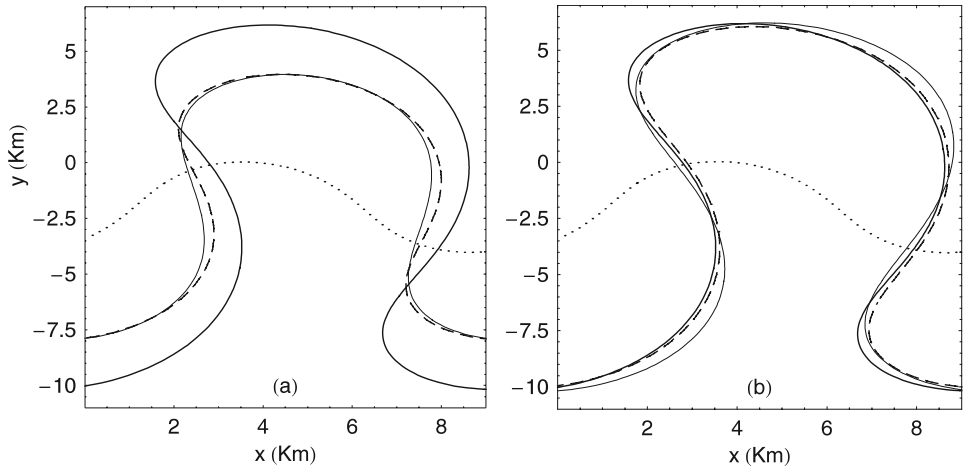

Figure 11. Evolution of the Kinoshita-shaped meander ($\theta = \pi/3$, dotted line) after 3000 years according to the ZS_4 (bold solid line), JP_2 (thin solid line), and IPS_U (dashed line) models. (a) Evolution using the same value of the erodibility coefficient ($E = 10^{-7}$).(b) Different erodibilities C_iE.

plotted). No significant hydraulic works were done in this reach (or in a relatively long tract upstream and downstream) during the considered temporal interval. As previously described in section 7.2, the erodibility coefficient E is evaluated for each model by visually fitting the simulated evolution to the real data, obtaining $E \times 10^7 = 2.0$, 1.5, and 0.9 for the IPS_U, JP_2, and ZS_4 models, respectively.

[80] The simulated planimetric evolutions are compared with the real evolution in Figure 13. The prediction by the ZS_4 model is remarkable, and the JP_2 model also seems to work quite well in spite of the fact that such models do not describe the bank erosion processes in detail and do not take into account external disturbances, such as soil heterogeneity, discharge variability, and riparian vegetation. The IPS_U model instead does not give good results. The reason for this is that the 1880 planform showed a weak multilobed pattern that disappeared during the river evolution presumably because of the mutual interaction between dominant and higher harmonics. In this case the capability of the second- and fourth-order models to force several harmonics allows the models to capture this aspect very well (especially the ZS_4 model). This capability is, instead, weak in the IPS_U model; therefore the modulation of the local wavelength is inhibited, and the multilobes cannot vanish. Therefore, while the IPS_U model can give satisfactory results for simple-shaped meanders (see the good amplitude responses shown in Figure 9), the presence of significant multilobes needs higher-order models in particular fourth-order ones.

8. ROLE OF EXTERNAL FORCING ON LONG-TERM RIVER DYNAMICS

[81] River morphodynamics can be studied according to a short- or long-term timescale. The former is typical of the evolution of single meanders before cutoff, while the latter spans times in which several cutoffs can occur [*Camporeale et al.*, 2005]. Such a distinction is fundamental as the long-term meandering dynamics are markedly affected by many external forcings, which can have considerable spatial and temporal variability and can interact with the long-term river dynamics themselves. Such factors may be both deterministic and stochastic and act in a multiplicative and additive way [*Perona et al.*, 2002].

[82] Taking advantage of the improvements that have been made in numerical analysis over the last 2 decades, the study of the long-term behavior of meandering river has been the subject of increasing attention by the scientific community. The recursive computation of the linear models discussed in the present review, along with an erosion law, has, in fact, allowed the planimetric migration of the rivers

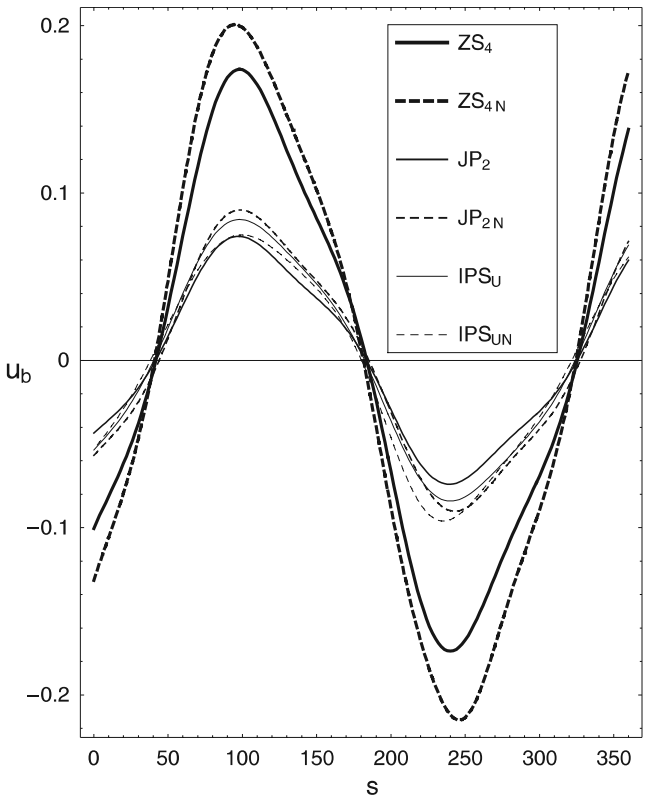

Figure 12. Comparisons of linear and nonlinear models.

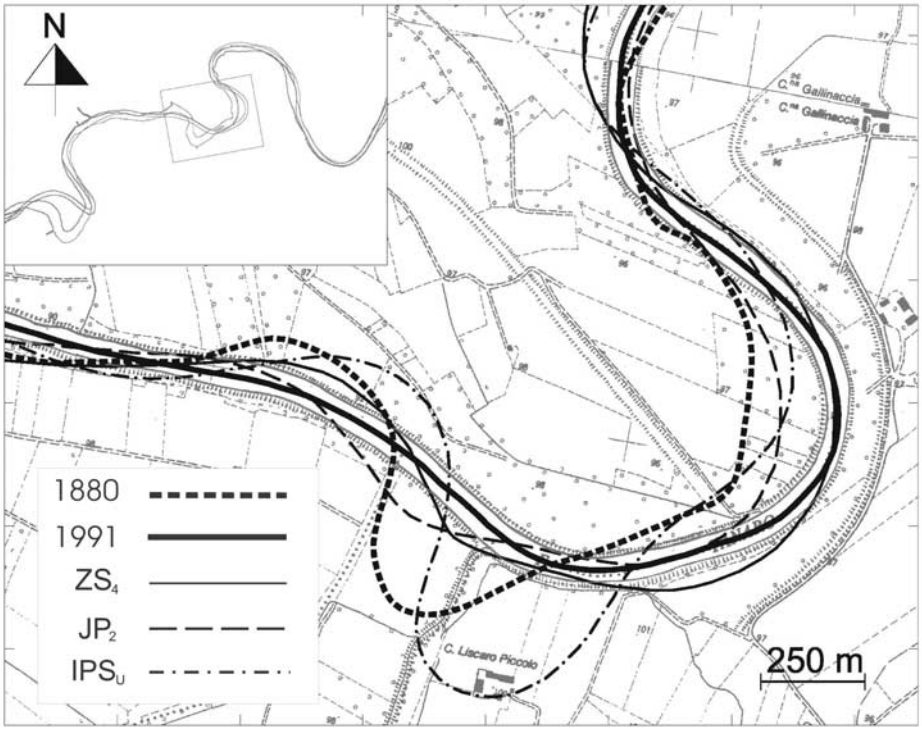

Figure 13. Comparison of the real river evolution of a reach of the Tanaro River and the evolutions simulated by the ZS_4 (thin solid line), JP_2 (thin dashed line), and IPS_U (dotted line) models. The bold dashed and solid lines mark the real river in 1880 and 1991, respectively.

spanning a timescale of the order of several thousands of years to be simulated step by step. In this context the study of the influence of different external forcings on meandering dynamics is becoming a promising topic, and the present section is a brief review of some recent contributions. We will focus in particular on four important factors that are able to influence long-term dynamics: cutoffs, sedimentation processes, riparian vegetation dynamics, and geological constraints.

8.1. Meander Cutoffs

[83] A cutoff event is an intermittent planimetric phenomenon dictated by nonlocal geometric conditions that eliminate the most mature meanders when two points of the river come into contact [*Gagliano and Howard*, 1984]. Cutoff behaves like an external action that sporadically forces the short-term meander evolution and affects the whole river planimetric dynamics in several ways. Using the IPS_U model, *Howard* [1984] recognized that cutoffs induce long-term statistical equilibrium of the spatial pattern. The same finding was confirmed by *Stølum* [1996] and *Howard* [1992] using JP_2 and by *Camporeale et al.* [2005] using ZS_4. Furthermore, *Stølum* [1996, 1997] suggested that cutoff avalanches are responsible for self-organized criticality, whereas *Howard* [1996] pointed out the role of chute cutoffs. Finally, although cutoff introduces a strong nonlinearity into temporal dynamics, it also seems to act as a "filter" that is able to limit the development of nonlinearities (induced by the nonlinear evolution equation (78)). This novel aspect, pointed out by *Perucca et al.* [2005], could justify the relative insensitivity of the statistics of long-term behavior to higher-order dynamical terms, which may be important in short-term evolution [*Camporeale et al.*, 2005].

8.2. Sedimentation Processes

[84] The physiographic features of the floodplain interact with a meandering river through two fundamental processes: point bar deposition and overbank sediment diffusion [*Howard*, 1992]. These aspects are of great importance in the characterization of the impermeable shale deposits that form oil reservoirs.

[85] The work by *Sun et al.* [1996] investigated the former aspect by developing long-term simulations of the IPS_U model and considering heterogeneous sedimentary environments. In particular, the erodibility coefficient, E, was determined from a map keeping track of the geological history. Different values of E were used for the virgin floodplain, the point bar deposits, and the cutoff deposits. The erodibility of the cutoff deposits was considered time-dependent, in a decreasing exponential way, in order to model the hardening due to the gradual filling of the oxbow lake by clay and silt and the successive formation of a clay plug. The authors pointed out that sedimentary heterogeneity leads to self-confinement of the meander belt, provided the timescale of the temporal decay of the oxbow lake erodibility is greater than the timescale of the longitudinal migration of meanders.

[86] In a subsequent work, *Sun et al.* [2001b] extended the analysis by using the JP_2 model along with the theory of

Parker and Andrews [1985] for the modeling of sediment sorting in bends. They were able to reproduce both the deposition of the coarse material in the upstream arms of the point bar and the deposition of fine material in the downstream part.

[87] As far as overbank sediment diffusion is concerned, it is worth mentioning the works by *Howard* [1992, 1996] again, where the JP_2 model was coupled with a deposition rate of fine sediments that exponentially decreased with the distance from the channel. The simulations reproduced zones of depression in the floodplain located in the axial position of the sharp meander bends on the downstream end of the point bar. Such thus formed sloughs were recognized to be consistent with the formations observed by *Lewin* [1978].

8.3. Dynamics of Riparian Vegetation

[88] The interactions between riparian vegetation and river morphodynamics are twofold: On the one hand, the river provides water, sediment, and seeds to the nearby riparian environment according its hydrological, hydraulic, and geomorphological characteristics [*Bendix and Hupp*, 2000]; on the other hand, vegetation uses water to live and to grow and significantly affects the hydraulic and geotechnical characteristics of the bed and banks, with an impact on the river morphodynamics [*Abernethy and Rutherfurd*, 1998]. In this sense, riparian vegetation can play both a passive and an active role in the dynamics [*Camporeale et al.*, 2006]. In the first case (i.e., passive role), vegetation merely affects roughness, hydraulic resistance, and bank erodibility in the same manner as any abiotic element with the same mechanical and morphological characteristics. In the second case, depending on the colonization, growth, and death processes, vegetation behaves as an active element of the ecological dynamics of the floodplain and interacts with the fluvial processes, leading to changes in the evolution of river patterns and, in turn, in the whole river-riparian vegetation system.

[89] In the context of meandering rivers the aforementioned processes induce the long-term formation of a ridge and swale topography with arcuate parallel bands of even aged trees [*Everitt*, 1968; *Nanson and Beach*, 1977]. Moreover, vegetation results are characterized by "a predictable development based on the distance of the river" [*Kalliola et al.*, 1992, p. 78] and a river-induced pattern with regular zonation of the communities [*Salo et al.*, 1986; *Puhakka and Kalliola*, 1995]. Although a quantitative physically based modeling of the long-term interactions between riparian vegetation and river meandering would be of paramount importance for the floodplain biogeomorphology [e.g., *Hughes* [1997], the models developed in literature are usually in a conceptual-qualitative form [e.g., *Bradley and Smith*, 1986; *McKenney et al.*, 1995; *Richter and Richter*, 2000]. In a recent work by *Perucca et al.* [2006] the IPS_U model has been coupled with a logistic model for the growth of riparian vegetation to simulate the effect of river planimetry on the vegetation pattern formation. Despite some crude approximations the numerical simulations highlighted the formation of an evident zone with low vegetation density in the internal part of the meanders in qualitative agreement with several real fluvial environments. Such promising results suggest improving and extending the previous approach to the modeling of the feedback of riparian vegetation on bank erosion and therefore on the planimetry evolution itself [e.g., *Perucca et al.*, 2007]. In this respect a first interesting model, at short-term timescales, has been numerically developed by *Van De Wiel and Darby* [2004] where the two-dimensional nonlinear equations for flow and sediment transport are coupled with a biogeotechnical bank stability analysis.

[90] Finally, we mention that riparian vegetation is also affected by the hyporheic exchange, as the oxygen flux from the stream regulates the redox conditions in the aquifer and the nutrient dynamics [*Jones and Mulholland*, 2000]. In this context, river sinuosity represents an important factor that regulates the structure of the intrameander hyporheic flow path (for an application using the ZS_4 model, see *Boano et al.* [2006]).

8.4. Geological Constraints

[91] Geological constraints can affect the planimetric evolution of meandering rivers in several different ways [e.g., *Watson et al.*, 1984]. Here we wish to focus on two particular cases: (1) tectonic lateral tilting of the floodplain and (2) the presence of valley walls with low erodibility. The first issue has been theoretically investigated by *Sun et al.* [2001c] by means of a modified version of the IPS_U model. In particular, the depth-averaged equation of the flow field was perturbed to consider both the effect of the lateral tilting and the effect of the curvature. The theory predicted a drift in the channel migration, moving toward lower (higher) elevations for high (small) Froude number.

[92] The second issue is particularly interesting whenever the distance between the valley walls is comparable to or smaller than twice the characteristic meander amplitude. In this case the lateral migration is remarkably confined, and the river planform is forced to assume a regular sequence of saw-toothed loops which migrate downstream. In this condition the neck cutoff process is also precluded at the long term. This point has been numerically investigated by *Howard* [1984, 1992, 1996] and *Sun et al.* [1996]. In all these works the simulated evolution of the planimetry, through the use of IPS_U or JP_2 models, allowed the typical patterns observable in nature to be reproduced, e.g., the well-known confined meanders of the Beaver River (Canada) [e.g., *Allen*, 1984].

9. CONCLUSIONS

[93] The work has investigated the significance of the main physical mechanisms involved in river meandering. To this aim we have reviewed and compared the fundamental existing linear models and several extensions thereof. These models have been hierarchically derived from a common and general mathematical framework. Moreover, a nonlinear version of each model has been derived with the aim of

assessing the effective influence of the nonlinearities that are neglected in the linear approach. A critical comparison of the models, a detailed discussion of the physical processes and the relevant hypotheses, and a comparison with real data have provided the following main results.

[94] The linear analysis has pointed out the importance of the closure of secondary currents. The amplitude of the response depends to a great extent on the modeling of the eddy viscosity. This aspect could justify the use of simplified models (e.g., IPS models) in practical applications, provided the secondary currents are modeled in detail [e.g., *Seminara and Solari*, 1998]. In contrast, the phase lag of secondary currents does not play a significant role, and although important from a theoretical point of view, the momentum redistribution due to the coupling between the main and the transverse flow only contributes weakly. Hence second-order models can reasonably be considered as good approximation tools for both predictive analysis and the computation of the resonant conditions. The analysis of higher harmonics, supported by the study of a real case, suggests that both fourth- and second-order models can give rise to multilobed planimetries, though fourth-order models are more accurate.

[95] The nonlinear analysis has pointed out that nonlinear models have a similar quantitative behavior as their linear counterparts. Such an agreement supports the use of linear theories to model the long-term evolution of meandering rivers [*Stølum*, 1996; *Howard*, 1992]. The phase response of both linear and nonlinear models is also similar, showing that one eigenvalue mainly controls the free response of the system.

[96] We conclude our work by pointing out that the evaluation of the effective significance of the different morphodynamic processes also has important implications for the simulation of meandering rivers in problems of riparian ecology [*Salo et al.*, 1986], geomorphology [*Howard*, 1992], oil research [*Swanson*, 1993], and river engineering [*Jansen et al.*, 1979]. Computational constraints or model complexity can, in fact, often induce one to choose the simplest meandering models. However, in the light of the results presented here, it is clear that the simplifications have to be adequate to the peculiar characteristics of each investigated problem.

APPENDIX A: VERTICAL DISTRIBUTIONS

[97] According to *Dean* [1974] the secondary currents can be modeled using a slowly varying eddy viscosity with the following vertical profiles

$$\Gamma = \frac{\kappa\zeta(1-\zeta)}{1+2A\zeta^2+3B\zeta^3} \tag{A1}$$

$$\mathcal{F} = \frac{C_f}{\kappa}\left[\ln\frac{\zeta}{\zeta_0} + A\left(\zeta^2-\zeta_0^2\right) + B\left(\zeta^3-\zeta_0^3\right)\right], \tag{A2}$$

where $A = 1.84$, $B = -1.56$, and κ is the von Karman constant. If a uniform eddy viscosity approach is used instead, the function $\mathcal{F}(\zeta)$ is obtained according to the *Engelund* [1974] slip velocity method, where the no-slip condition on the bottom is replaced by

$$\frac{u^*}{u_f} = 2 - 2.5\ln\zeta_0 \quad v^* = \frac{u^*}{u_f}\alpha v^*_{,z} \quad (z=\eta) \tag{A3}$$

in which u_f is the friction velocity. This allows an analytic evaluation of the coefficient $a^{(i)}$ and functions G_i to be made, whose expressions are

$$\Gamma = \alpha, \quad \mathcal{F} = 1 - \frac{\varepsilon}{\alpha}\left(\frac{1}{2}\zeta^2 - \zeta + \frac{1}{2}\right), \quad \varepsilon = \sqrt{C_f}, \tag{A4}$$

$$G_0 = \sum_{j=1}^{3}\frac{g_{0j}\varepsilon^j}{\alpha^{j+1}}, \quad G_1 = \sum_{j=1}^{5}\frac{g_{1j}\varepsilon^j}{\alpha^{j+2}}, \quad G_2 = \sum_{j=1}^{5}\frac{g_{2j}\varepsilon^j}{\alpha^{j+2}}, \tag{A5}$$

$$a^{(0)} = \sum_{i=0}^{3}\frac{a_{0i}\varepsilon^i}{\alpha^i}, \quad a^{(1)} = \sum_{i=2}^{5}\frac{a_{1i}\varepsilon^i}{\alpha^{i+1}}, \quad a^{(2)} = \sum_{i=1}^{5}\frac{a_{2i}\varepsilon^i}{\alpha^{i+1}}, \tag{A6}$$

$$g_{ij} = \sum_{k=0}^{n_{ij}} g_{ijk}\zeta^k. \tag{A7}$$

The numerical coefficients a_{ij}, n_{ij}, and g_{ijk} are reported in the auxiliary material[1].

APPENDIX B: COEFFICIENTS FOR THE FOURTH-ORDER MODELS

[98] Starting from the system of partial differential equations (45)–(48) and by means the Fourier decomposition in the lateral coordinate, *Zolezzi and Seminara* [2001] obtained m systems of ODEs that can be written in the algebraic form

$$\mathbf{A_4}x_{,s} + \mathbf{B_4}x = A_m\mathbf{\Omega}\boldsymbol{\kappa}(s), \tag{B1}$$

where

$$\mathbf{A_4} = \begin{bmatrix} 1 & 0 & 1 & 0 \\ 0 & 1 & 0 & 0 \\ 1 & 0 & 0 & 0 \\ a_4 & 0 & 0 & a_5 \end{bmatrix}, \tag{B2}$$

$$\mathbf{B_4} = \begin{bmatrix} a_1 & 0 & 0 & a_2 \\ 0 & a_3 & M & 0 \\ 0 & -M & 0 & M \\ 0 & -M & F_0^2 a_6 M^2 & -M^2 a_6 \end{bmatrix}, \tag{B3}$$

$$\boldsymbol{\kappa} = \left\{\mathcal{C}, \mathcal{C}_{,s}, \mathcal{C}_{,ss}, \mathcal{C}_{,sss}\right\}^T, \tag{B4}$$

[1]Auxiliary materials are available in the HTML. doi:10.1029/2005RG000185.

whereas the vector $x = \{u_m, v_m, h_m, d_m\}^T$ contains the Fourier coefficients of the unknowns $\{u, v, h, d\}^T$ and the elements of the matrix $\mathbf{\Omega}$ read

$$\Omega_{11} = b_1 - a_2\left(F_0^2 b_2 - b_4\right), \tag{B5}$$

$$\Omega_{12} = -b_2 - a_2\left(F_0^2 b_3 - b_6\right), \quad \Omega_{13} = -b_3 - F_0^2 a_2 b_5, \tag{B6}$$

$$\Omega_{14} = -b_5, \quad \Omega_{32} = b_4 - F_0^2 b_2, \tag{B7}$$

$$\Omega_{33} = b_6 - F_0^2 b_3, \quad \Omega_{34} = -F_0^2 b_5, \tag{B8}$$

$$\Omega_{42} = a_5\left(b_4 - F_0^2 b_2\right), \tag{B9}$$

$$\Omega_{43} = a_5\left(b_6 - F_0^2 b_3\right), \quad \Omega_{44} = F_0^2 a_5 b_5, \tag{B10}$$

$$\Omega_{21} = \Omega_{22} = \Omega_{23} = \Omega_{24} = \Omega_{31} = \Omega_{41} = 0. \tag{B11}$$

The Laplace transform of (B1) gives

$$[\tau\mathbf{A_4} + \mathbf{B_4}]\hat{\mathbf{x}}(\tau) = A_m\mathbf{\Omega}\mathcal{K}\hat{\mathcal{C}}(\tau), \tag{B12}$$

where τ is the complex variable, the hat refers to the transformed variables, and $\mathcal{K} = \{1, \tau, \tau^2, \tau^3\}^T$. Hence, defining $\mathbf{K} = \tau\mathbf{A_4} + \mathbf{B_4}$ and $\mathcal{L}_4 = A_m\mathbf{\Omega}\mathcal{K}$ and using Cramer's rule, we obtain the coefficients σ of the homogeneous part of the fourth-order differential equation (53) by collecting the coefficients of the characteristic polynomial det [$\mathbf{K}$]

$$\sigma_0 = \epsilon M^2 a_1 a_6, \tag{B13}$$

$$\sigma_1 = \epsilon\big[M^2 a_6 + a_2(a_4 - 1) + a_1(1 - a_5) + F_0^2 a_3 a_6(a_1 - a_2)\big], \tag{B14}$$

$$\sigma_2 = \epsilon\big[1 - a_5 + F_0^2 a_6(a_1 - a_2 + a_3) - a_3 a_6\big], \tag{B15}$$

$$\sigma_3 = \epsilon\left(F_0^2 - 1\right)a_6 - a_3, \tag{B16}$$

where $\epsilon = M^2/(a_5 - a_4)$. Similarly, the coefficients ρ of the nonhomogeneous part are given by the characteristic polynomial det [$\mathbf{K}^1_{\mathcal{L}}$] where the notation $\mathbf{K}^1_{\mathcal{L}}$ refers to the matrix $\mathbf{K}$ with the first column replaced by the vector $\mathcal{L}$. Therefore the coefficients of equation (53) read

$$\rho_1 = \epsilon M^2 a_6\left(b_1 - F_0^2 b_2 a_2 + b_4 a_2\right), \tag{B17}$$

$$\rho_2 = \epsilon\left\{\left(1 - a_5 + F_0^2 a_3 a_6\right)b_1 - M^2 a_6 \cdot \left[b_2 + a_2\left(F_0^2 b_3 - b_6\right)\right]\right\}, \tag{B18}$$

$$\rho_3 = \epsilon[(a_5 - 1)b_2 + a_6\left(F_0^2 b_1 - M^2 b_3 - a_3 b_4 - F_0^2 M^2 a_2 b_5\right)], \tag{B19}$$

$$\rho_4 = \epsilon\left[(a_5 - 1)b_3 - a_6\left(b_4 + M^2 b_5 + a_3 b_6\right)\right], \tag{B20}$$

$$\rho_5 = \epsilon[(a_5 - 1)b_5 - a_6 b_6], \quad \rho_6 = \rho_7 = 0. \tag{B21}$$

[99] It should be noticed that the coefficients of the differential equations that describe v_m, h_n, and d_m can easily be obtained following the same procedure described above. The only difference concerns the coefficients ρ of the nonhomogeneous part. These are given by the characteristic polynomial det [$\mathbf{K}^i_{\mathcal{L}}$], where i refers to the ith column which has to be substituted (with $i = 2$, 3, and 4 correspondent to v_m,h_n, and d_m, respectively).

APPENDIX C: COEFFICIENTS FOR THE SECOND-ORDER MODELS

[100] Reducing the procedure of Appendix B to a two-dimensional vectorial space, the coefficients of the second-order models can be obtained as

$$\sigma_0 = -\varsigma\left(a_6 a_1 M^2\right), \quad \sigma_1 = \varsigma\left[a_2(1 - a_4) - a_6 M^2\right] + a_1, \tag{C1}$$

$$\rho_1 = \varsigma\left[a_6 M^2(a_2 b_4 - b_1)\right], \tag{C2}$$

$$\rho_2 = b_1 - a_6 M^2\left(b_1^{(1)} - a_2 b_6\right), \tag{C3}$$

$$\rho_3 = b_1^{(1)} - \varsigma a_6 M^2 b_1^{(2)}, \quad \rho_4 = b_1^{(2)}, \quad \varsigma = (a_5 - 1)^{-1}. \tag{C4}$$

In order to obtain the ZS_2 model we have corrected a small algebraic mistake that affects the expression of h_0 given by *Zolezzi and Seminara* [2001]. However, this mistake does not compromise the subsequent results of Zolezzi and Seminara as the analytical expression of the superelevation induced by the curvature is not used in the ZS_4 model.

GLOSSARY

Bar: Two-dimensional perturbation of the riverbed topography occurring on a megascale, namely, of the order of the channel width [*Colombini et al.*, 1987]. Free bars (also called alternate bars) are induced by flow bottom instability and present long stream migration [*Tubino et al.*, 1999], whereas forced (or point) bars are stationary and are driven by the curvature-induced secondary flow.

Cutoff: Bypass of a meander loop in favor of a shorter path and the following formation of an abandoned reach, called oxbow lake. If cutoff takes place to avoid the self-intersection of two reaches that come into contact, it is called "neck cutoff"; otherwise, cutoff is known as "chute."

Kinoshita curve: A theoretical meandering curve named after the Japanese geomorphologist who corrected the sine-generated curve proposed by *Langbein and Leopold* [1966] with two additional third-order harmonics to give equation (79). In this way it is possible to model not only the characteristic ''fattening'' of meanders (already accounted for by the sine-generated curve) but also the ubiquitous ''skewing'' of the loops [*Parker et al.*, 1982]. Subsequently, *Seminara et al.* [1994] showed that the absence of even harmonics in the Kinoshita curve can be justified by the cubic nonlinearity of the evolution equation (78). They also showed that the eventual formation of higher harmonics than the third is precluded by cutoff occurrence.

Overdeepening phenomenon: ''Spatial transient whereby the scour associated with the point bar configuration establishes in a bend of constant curvature downstream of a straight reach'' [*Zolezzi et al.*, 2005, p. 192].

Planimetry: Two-dimensional path of the river axis curve.

Superelevation: Outward increase of the water surface induced by stream curvature.

[101] **ACKNOWLEDGMENTS.** The authors are grateful to reviewers for their useful comments. Finally, we would like to thank the Regione Piemonte, the Cassa di Risparmio di Cuneo (CRC), and the Cassa di Risparmio di Torino (CRT) foundations for their financial support.

[102] The Editor responsible for this paper was Daniel Tartakovsky. He thanks reviewer Sergio Fagherazzi and one anonymous cross-disciplinary reviewer.

REFERENCES

Abernethy, B., and I. D. Rutherfurd (1998), Where along a river's length will vegetation most effectively stabilise stream banks?, *Geomorphology*, *23*, 55–75.

Allen, J. R. L. (1965), A review of the origin and characteristics of recent alluvial sediments, *Sedimentology*, *5*, 89–191.

Allen, J. R. L. (1970), A quantitative model of grain size and sedimentary structures in lateral deposits, *J. Geol.*, *7*, 129–146.

Allen, J. R. L. (1984), *Sedimentary Structures: Their Character and Physical Basis*, Elsevier, New York.

Beck, S., D. A. Melfi, and K. Yalamanchili (1984), Lateral migration of the Genesses River, New York, in *River Meandering*, edited by C. M. Elliott, pp. 510–517, Am. Soc. of Civ. Eng., Reston, Va.

Bendix, J., and C. R. Hupp (2000), Hydrological and geomorphological impacts on riparian plant communities, *Hydrol. Processes*, *14*, 2977–2990.

Blanckaert, K., and H. J. De Vriend (2003), Nonlinear modeling of mean flow redistribution in curved open channel bends, *Water Resour. Res.*, *39*(12), 1375, doi:10.1029/2003WR002068.

Blanckaert, K., and H. J. De Vriend (2004), Secondary flow in sharp open-channel bends, *J. Fluid Mech.*, *498*, 353–380.

Blondeaux, P., and G. Seminara (1985), A unified bar-bend theory of river meanders, *J. Fluid Mech.*, *157*, 449–470.

Boano, F., C. Camporeale, R. Revelli, and L. Ridolfi (2006), Sinuosity-driven hyporheic exchange in meandering rivers, *Geophys. Res. Lett.*, *33*, L18406, doi:10.1029/2006GL027630.

Bradley, C. E., and D. G. Smith (1986), Plains cottonwood recruitment and survival on a prairie meandering river floodplain, Milk River, southern Alberta and northern Montana, *Can. J. Bot.*, *64*, 1433–1442.

Bridge, J. (1992), A revised model for water flow, sediment transport, bed topography and grain size sorting in natural river bends, *Water Resour. Res.*, *28*, 999–1013.

Brower, R. C., D. A. Kessler, J. Koplik, and H. Levine (1984), Geometrical models of interface evolution, *Phys. Rev. A*, *29*, 1335–1342.

Callander, R. A. (1978), River meandering, *Annu. Rev. Fluid Mech.*, *10*, 129–158.

Camporeale, A., and L. Ridolfi (2006), Convective nature of the planimetric instability in meandering river dynamics, *Phys. Rev. E*, *73*(2), doi:10.1103/PhysRevE.73.026311.

Camporeale, C., P. Perona, A. Porporato, and L. Ridolfi (2005), On the long-term behavior of meandering rivers, *Water Resour. Res.*, *41*, W12403, doi:10.1029/2005WR004109.

Camporeale, C., P. Perona, and L. Ridolfi (2006), Hydrological and geomorphological significance of riparian vegetation in arid regions, in *Dryland Ecohydrology*, edited by P. D'Odorico and A. Porporato, Springer, New York.

Carson, M. A., and M. F. Lapointe (1983), The inherent asymmetry of river meander planform, *J. Geol.*, *91*, 41–55.

Chitale, S. V. (1970), River channel patterns, *J. Hydraul. Div. Am. Soc. Civ. Eng.*, *96*, 201–221.

Colombini, M., G. Seminara, and M. Tubino (1987), Finite amplitude alternate bars, *J. Fluid Mech.*, *181*, 213–232.

Crosato, A. (1987), Simulation model of meandering processes of rivers, paper presented at Euromech 215 Conference, Univ. of Genoa, Genoa, Italy.

Crosato, A. (1989), Meander migration prediction, *Excerpta*, *4*, 169–198.

Cross, M. C., and P. C. Hohenberg (1993), Pattern formation outside of equilibrium, *Rev. Mod. Phys.*, *65*(3), 851–1112.

Darby, S. E., A. M. Alabyn, and M. J. Van de Wiel (2002), Numerical simulation of bank erosion and channel migration in meandering rivers, *Water Resour. Res.*, *38*(9), 1163, doi:10.1029/2001WR000602.

Dean, R. B. (1974), Reynolds number dependence on skin friction in two dimensional rectangular duct flow and a discussion on the 'law of the wake', *Aero. Rep. 74-11*, Imperial Coll., London.

De Vries, M. (1965), Considerations about non-steady bed-load transport in open channels, paper presened at 11th Congress, Int. Assoc. for Hydraul. Res., Leningrad, Russia.

Dietrich, W. E., and J. D. Smith (1983), Influence of point bar on flow through meander bends, *Water Resour. Res.*, *19*, 1173–1192.

Dietrich, W. E., J. D. Smith, and T. Dunne (1979), Flow and sediment transport in a sand bedded meander, *J. Geol.*, *87*, 305–315.

Do Carmo, M. (1976), *Differential Geometry of Curves and Surface*, Prentice-Hall, Upper Saddle River, N. J.

Duan, J. G., and P. Y. Julien (2005), Numerical simulation of the inception of channel meandering, *Earth Surf. Processes Landforms*, *30*(9), 1093–1110.

Duan, J. G., S. S. Y. Wang, and Y. Jia (2001), The application of the enhanced CCHE2D model to study the alluvial channel migration processes, *J. Hydraul. Res.*, *39*, 1–12.

Edwards, B. F., and D. H. Smith (2002), River meandering dynamics, *Phys. Rev. E*, *65*(4), doi:10.1103/PhysRevE.65.046303.

Elliott, C. M., (Ed.) (1984), *River Meandering*, Am. Soc. of Civ. Eng., Reston, Va.

Engelund, F. (1974), Flow and topography in channel bends, *J. Hydraul. Eng. Div. Am. Soc. Civ. Eng.*, *11*, 1631–1648.

Engelund, F. (1981), The motion of sediment particles on an inclined bed, *Tech. Rep. 53*, Inst. of Hydrodyn. and Hydraul. Eng., Tech. Univ. of Denmark, Copenhagen.

Everitt, B. (1968), Use of the cottonwood in an investigation of the recent history of a floodplain, *Am. J. Sci.*, *266*, 417–439.

Exner, F. M. (1925), Uber Die Wechselwirkung Zwischen Wasser und Geschiebe in Flussen, *Sitzungsber. Akad. Wiss. Vien Math. Naturwiss. Kl., Abt. 2A*, *134*, 165–180.

Ferguson, R. I., D. R. Parsons, S. N. Lane, and R. J. Hardy (2003), Flow in meander bends with recirculation at the inner banks, *Water Resour. Res.*, *39*(11), 1322, doi:10.1029/2003WR001965.

Friedkin, J. F. (1945), A laboratory study of the meandering of alluvial rivers, report, Miss. River Comm., U.S. Army Corps of Eng., Vicksburg, Miss.

Gagliano, S. M. and P. C. Howard (1984), The neck cutoff oxbow lake along the lower Mississippi River, in *River Meandering*, edited by C. M. Elliot, pp. 147–158, Am. Soc. of Civ. Eng., Reston, Va.

Garcia, M., and Y. Nino (1993), Dynamics of sediment bars in straight and meandering channels: Experiment on the resonance phenomenon, *J. Hydraul. Res.*, *31*, 739–761.

Gottlieb, M. (1976), Three dimensional flow pattern and bed topography in meandering channels, *Ser. Pap. 11*, Inst. of Hydrodyn. and Hydraul. Eng., Tech. Univ. of Denmark, Copenhagen.

Hasegawa, K. (1989), Universal bank erosion coefficient for meandering rivers, *J. Hydraul. Eng.*, *115*, 744–765.

Hasegawa, K., K. Nakamura, and T. Toyabe (1998), Analysis of experimental bed topography data with resonance conditions in meandering channels using linear theories, *J. Hydrosci. Hydraul. Eng.*, *16*, 73–86.

Henderson, F. M. (1966), *Open Channel Flow*, Macmillan, New York.

Howard, A. D. (1984), Simulation model of meandering, in *River Meandering*, edited by C. M. Elliott, pp. 952–963, Am. Soc. of Civ. Eng., Reston, Va.

Howard, A. D. (1992), Modeling channel migration and floodplain sedimentation in meandering streams, in *Lowland Floodplain Rivers: Geomorphological Perspectives*, edited by P. A. Carling and G. E. Petts, pp. 1–41, John Wiley, Hoboken, N. J.

Howard, A. D. (1996), Modelling channel evolution and floodplain morphology, in *Floodplain Processes*, edited by M. G. Anderson, D. E. Walling, and P. D. Bates, pp. 15–62, John Wiley, Hoboken, N. J.

Howard, A. D., and A. T. Hemberger (1991), Multivariate characterization of meandering, *Geomorphology*, *4*, 161–186.

Hughes, F. M. R. (1997), Floodplain biogeomorphology, *Prog. Phys. Geogr.*, *21*, 501–529.

Ikeda, S. (1982), Lateral bed load transport on side slopes, *J. Hydraul. Eng. Div. Am. Soc. Civ. Eng.*, *108*, 1369–1373.

Ikeda, S., and T. Nishimura (1986), Flow and bed profile in meandering sand-silt rivers, *J. Hydraul. Eng.*, *112*, 562–579.

Ikeda, S. and G. Parker (Eds.) (1989), *River Meandering*, *Water Resour. Monogr.*, vol. 12, AGU, Washington, D. C.

Ikeda, S., M. Yamasaka, and M. Chiyoda (1987), Bed topography and sorting in bends, *J. Hydraul. Eng.*, *113*, 190–206.

Ikeda, S. G., G. Parker, and K. Sawai (1981), Bend theory of river meanders, 1, Linear development, *J. Fluid Mech.*, *112*, 363–377.

Imran, J., G. Parker, and C. Pirmez (1999), A nonlinear model of flow in meadering submarine and subaerial channels, *J. Fluid Mech.*, *400*, 295–331.

Jansen, P., L. Van Bendegom, J. Van Den Berg, M. de Vries, and A. Zanen (1979), *Principles of River Engineering: The Non-Tidal Alluvial River*, Pitman, London.

Johannesson, H. and G. Parker (1989a), Linear theory of river meanders, in *River Meandering*, *Water Resour. Monogr.*, vol. 12, edited by S. Ikeda and G. Parker, pp. 181–214, AGU, Washington, D. C.

Johannesson, H., and G. Parker (1989b), Secondary flow in a mildly sinuous channel, *J. Hydraul. Eng.*, *115*, 289–308.

Johannesson, H., and G. Parker (1989c), Velocity redistribution in meandering rivers, *J. Hydraul. Eng.*, *115*, 1019–1037.

Jones, J. B. and P. J. Mulholland (2000), *Streams and Ground Waters*, Elsevier, New York.

Kalkwijk, J. P. T., and H. J. De Vriend (1980), Computation of the flow in shallow river bends, *J. Hydraul. Res.*, *18*, 327–342.

Kalliola, R., J. Salo, M. Puhakka, and M. Rajasilta (1992), Upper Amazon channel migration, *Naturwissenshaften*, *79*, 75–79.

Kennedy, J. F., T. Nakato, and A. J. Odgaard (1984), Analysis, numerical modeling, and experimental investigation of flow in river bends, in *River Meandering, Conference Rivers 1983, New Orleans*, edited by C. M. Elliott, pp. 843–856, Am. Soc. of Civ. Eng., Reston, Va.

Keylock, C. J., R. J. Hardy, D. R. Parsons, R. I. Ferguson, S. N. Lane, and K. S. Richards (2005), The theoretical foundations and potential for large-eddy simulation (LES) in fluvial geomorphic and sedimentological research, *Earth Sci. Rev.*, *71*(3–4), 271–304.

Kikkawa, H., S. Ikeda, and A. Kitagawa (1976), Flow and bed topography in curved open channels, *J. Hydraul. Div. Am. Soc. Civ. Eng.*, *102*, 1327–1342.

Kinoshita, R. (1961), Investigation of channel deformation in Ishikari River, *Tech. Rep. 13*, 174 pp., Dep. Sci. and Tech., Bur. of Resour., Tokyo, Japan.

Kinoshita, R., and H. Miwa (1974), River channel formation which prevents downstream translation of transverse bars (in Japanese), *Shinsabo*, *94*, 12–17.

Kitanidis, P. K., and J. F. Kennedy (1984), Secondary current and river meander formation, *J. Fluid Mech.*, *144*, 217–229.

Kovacs, A., and G. Parker (1994), A new vectorial bedload formulation and its application to the time evolution of straight river channels, *J. Fluid Mach.*, *267*, 153–183.

Lancaster, S. T., and R. L. Bras (2002), A simple model of river meandering and its comparision to natural channels, *Hydrol. Processes*, *16*, 1–26.

Langbein, W. B., and L. B. Leopold (1966), River meanders—Theory of minimum variance, *U.S. Geol. Surv. Prof. Pap.*, *422H*, 1–19.

Lanzoni, S., A. Siviglia, A. Frascati, and G. Seminara (2006), Long waves in erodible channels and morphodynamic influence, *Water Resour. Res.*, *42*, W06D17, doi:10.1029/2006WR004916.

Leopold, L. B., and M. G. Wolman (1960), River meanders, *Bull. Geol. Soc. Am.*, *71*, 769–794.

Lewin, L. (1978), Meander development and floodplain sedimentation: A case study from mid-Wales, *Geol. J.*, *13*, 25–36.

Ligget, J. A. (1994), *Fluid Mechanics*, McGraw-Hill, New York.

Liverpool, T. B., and S. F. Edwards (1995), Dynamics of a meandering river, *Phys. Rev. Lett.*, *75*(16), 3016–3019.

McKenney, R., R. B. Jacobson, and R. C. Wertheimer (1995), Woody vegetation and channel morphogenesis in low-gradient, gravel-bed streams in the Ozark Plateaus, Missouri and Arkansas, *Geomorphology*, *13*, 175–198.

Mosselman, E. (1991), Modelling of river morphology with non-orthogonal horizontal coordinates, *Commun. Hydraul. Geotech. Eng. 91-1*, Delft Univ. of Technol., Delft, Netherlands.

Mosselman, E. (1998), Morphological modelling of rivers with erodible banks, *Hydrol. Processes*, *12*, 1357–1370.

Mosselman, E., and A. Crosato (1991), Universal bank erosion coefficient for meandering rivers, *J. Hydraul. Eng.*, *117*, 942–943.

Nakayama, K., H. Segur, and M. Wadati (1992), Integrability and the motion of curves, *Phys. Rev. Lett.*, *69*(18), 2603–2606.

Nanson, G. C., and H. F. Beach (1977), Forest succession and sedimentation on a meandering-river floodplain, north east British Columbia, Canada, *J. Biogeogr.*, *4*, 229–251.

Nanson, G. C., and E. J. Hickin (1983), Channel migration and incision on the Beatton River, *J. Hydraul. Eng.*, *109*, 327–337.

Nelson, J. and J. Smith (1989a), Evolution and stability of erodibel channel beds, in *River Meandering*, edited by S. Ikeda and G. Parker, *Water Resour. Monogr.*, vol. 12, pp. 321–377, AGU, Washington D. C.

Nelson, J. M. and J. D. Smith (1989b), Flow in meandering channel with natural topography, in *River Meandering*, edited by S. Ikeda and G. Parker, *Water Resour. Monogr.*, vol. 12, pp. 69–102, AGU, Washington, D. C.

Nezu, I. and H. Nakagawa (1993), *Turbulence in Open-Channel Flows*, A. A. Balkema, Brookfield, Vt.

Odgaard, A. J. (1982), Bed characteristics in alluvial channel bends, *J. Hydraul. Div. Am. Soc. Civ. Eng.*, *108*, 1268–1281.

Odgaard, A. J. (1986), Meander flow model. I: Development, *J. Hydraul. Eng.*, *112*, 1117–1136.

Odgaard, A. J., and M. A. Bergs (1988), Flow processes in curved alluvial channel, *Water Resour. Res.*, *24*, 45–56, (Correction, *Water Resour. Res.*, *25*, 2397, 1989).

Odgaard, A. J. and J. F. Kennedy (1982), Analysis of Sacramento River bend flows, and development of a new method for bank protection, *IIHR Rep. 241*, Iowa Inst. of Hydraul. Res., Univ. of Iowa, Iowa City.

Olsen, K. W. (1987), Bed topography in shallow river bends, *Commun. Hydraul. Geotech. Eng. 87-1*, Delft Univ. of Technol., Delft, Netherlands.

Olsen, N. R. B. (2003), Three dimensional CFD modeling of self forming meandering channel, *J. Hydraul. Eng.*, *129*, 366–372.

Parker, G. (1976), On the cause and characteristic scales of meandering and braiding in rivers, *J. Fluid Mech.*, *76*, 457–483.

Parker, G., and E. D. Andrews (1985), Sorting of bed load sediment by flow in meander bends, *Water Resour. Res.*, *21*, 1361–1373.

Parker, G., and E. D. Andrews (1986), On the time development of meanders bends, *J. Fluid Mech.*, *162*, 139–156.

Parker, G. and H. Johannesson (1989), Observations on several recent theories of resonance and overdeepening in meandering channels, in *River Meandering*, *Water Resour. Monogr.*, vol. 12, edited by S. Ikeda and G. Parker, pp. 379–415, AGU, Washington, D. C.

Parker, G., K. Sawai, and S. Ikeda (1982), Bend theory of river meanders. part 2. Nonlinear deformation of finite-amplitude bends, *J. Fluid Mech.*, *115*, 303–314.

Parker, G., P. Diplas, and J. Akiyama (1983), Meander bends of high amplitude, *J. Hydraul. Eng.*, *109*, 1323–1337.

Partheniades, E. (1965), Erosion and deposition of cohesive soils, *J. Hydraul. Div. Am. Soc. Civ. Eng.*, *91*, 105–139.

Partheniades, E., and R. R. Paaswell (1970), Erodibility of channels with cohesive boundaries, *J. Hydraul. Div. Am. Soc. Civ. Eng.*, *96*, 755–771.

Perona, P., A. Porporato, and L. Ridolfi (2002), River dynamics after cutoff: A discussion of different approaches, in *Proceedings of the River Flow 2002 International Conference on Fluvial Hydraulics*, edited by D. Bousmar and Y. Zech, pp. 715–721, Int. Assoc. for Hydraul. Res., Delft, Netherlands.

Perucca, E., C. Camporeale, and L. Ridolfi (2005), Nonlinear analysis of the geometry of meandering rivers, *Geophys. Res. Lett.*, *32*, L03402, doi:10.1029/2004GL021966.

Perucca, E., C. Camporeale, and L. Ridolfi (2006), Influence of river meandering dynamics on riparian vegetation pattern formation, *J. Geophys. Res.*, *111*, G01001, doi:10.1029/2005JG000073.

Perucca, E., C. Camporeale, and L. Ridolfi (2007), Significance of the riparian vegetation dynamics on meandering river morphodynamics, *Water Resour. Res.*, doi:10.1029/2006WR005234, in press.

Pizzuto, J., and T. Meckelnburg (1989), Evaluation of a linear bank erosion equation, *Water Resour. Res.*, *25*, 1005–1013.

Puhakka, M., and R. Kalliola (1995), Floodplain vegetation mosaics in western Amazonia, *Biogeographica*, *71*, 1–14.

Richardson, K. R. (2002), Simplified model for assessing meander bends migration rates, *J. Hydraul. Eng.*, *128*, 1094–1097.

Richter, B. D., and H. E. Richter (2000), Prescribing flood regimes to sustain riparian ecosystem along meandering rivers, *Conserv. Bio.*, *14*, 1467–1478.

Robinson, S. K. (1991), Coherent motions in the turbulent boundary layer, *Annu. Rev. Fluid Mech.*, *23*, 601–639.

Rozowskij, I. L. (1957), *Flow of Water in Bends of Open Channel*, Acad. Sci., Kiev, Ukraine.

Rüther, N., and N. R. B. Olsen (2005), Three-dimensional modelling of sediment transport in a narrow 90° channel bend, *J. Hydraul. Eng.*, *131*, 917–920.

Salo, J., R. Kalliola, I. Hakkinen, Y. Makinen, P. Niemela, M. Puhakka, and P. Coley (1986), River dynamics and the diversity of Amazon lowland forest, *Nature*, *322*, 254–258.

Seminara, G. (1998), Stability and morphodynamics, *Meccanica*, *33*, 59–99.

Seminara, G. (2006), Meanders, *J. Fluid Mech*, *554*, 271–297.

Seminara, G., and L. Solari (1998), Finite amplitude bed deformations in totally and partially transporting wide channel, *Water Resour. Res.*, *34*, 1585–1594.

Seminara, G. and M. Tubino (1985), Further results on the effect of transport in suspension on flow in weakly meandering channels, in *Colloquium on the Dynamics of Alluvial Rivers*, pp. 67–112, Univ. of Genoa, Genoa, Italy.

Seminara, G. and M. Tubino (1989), Alternate bars and meandering, in *River Meandering*, *Water Resour. Monogr.*, vol. 12, edited by S. Ikeda and G. Parker, pp. 267–320, AGU, Washington, D. C.

Seminara, G., and M. Tubino (1992), Weakly nonlinear theory of regular meanders, *J. Fluid Mech.*, *244*, 257–288.

Seminara, G., M. Tubino, and D. Zardi (1994), Planimetric evolution of meandering rivers from incipient formation to cutoff (in Italian), in *XXIV Convegno Di Idraulica e Costruzioni Idrauliche, Napoli, 20–22 Settembre*, vol. 2-T4, pp. 207–218, CNR, Naples, Italy.

Seminara, G., G. Zolezzi, M. Tubino, and D. Zardi (2001), Downsream and upstream influence in river meandering. part 2. Planimetric development, *J. Fluid. Mech.*, *438*, 213–230.

Shimizu, Y., H. Yamuguchi, and T. Itakura (1990), Three-dimensional computation of flow and bed deformation, *J. Hydraul. Eng.*, *116*, 1090–1108.

Shimizu, Y., M. Tubino, and Y. Watanabe (1992), Numerical calculations of bed deformation in a range of resonant wavenumbers in meandering channels, *Proc. Hydraul. Eng. ASCE*, *36*, 15–22.

Smith, D., and S. R. McLean (1984), A model of flow in meandering streams, *Water Resour. Res.*, *20*, 1301–1315.

Stølum, H. H. (1996), River meandering as a self-organized process, *Science*, *271*, 1710–1713.

Stølum, H. H. (1997), Fluctuations at the self-organized critical state, *Phys. Rev. E*, *56*(6), 6710–6718.

Struiksma, N., K. Olesen, C. Flokstra, and H. De Vriend (1985), Bed deformation in curved alluvial channels, *J. Hydraul. Res.*, *23*, 57–79.

Sun, T., T. Jøssang, P. Meakin, and K. Schwarz (1996), A simulation model for meandering rivers, *Water Resour. Res.*, *32*, 2937–2954.

Sun, T., P. Meakin, and T. Jøssang (2001a), A computer model for meandering rivers with multiple bed load sediment size: 1. Theory, *Water Resour. Res.*, *37*, 2227–2241.

Sun, T., P. Meakin, and T. Jøssang (2001b), A computer model for meandering rivers with multiple bed load sediment size: 2. Computer simulations, *Water Resour. Res.*, *37*, 2243–2258.

Sun, T., P. Meakin, and T. Jssang (2001c), Meander migration and the lateral tilting of floodplains, *Water Resour. Res.*, *37*, 1485–1502.

Swanson, D. C. (1993), The importance of fluvial processes and related reservoir deposits, *JPT J. Pet. Technol.*, *45*(4), 368–377.

Talmon, A. M., N. Struiksma, and M. C. L. M. Van Mierlo (1995), Laboratory measurements of the directions of sediment transport on transverse alluvial-bed slopes, *J. Hydraul. Res.*, *33*, 495–517.

Thorne, S. D., and D. J. Furbish (1995), Influence of coarse bank roughness on flow within a sharply curved river bend, *Geomorphology*, *12*, 241–257.

Tubino, M., and G. Seminara (1990), Free-forced interactions in developing meanders and suppression of free bars, *J. Fluid Mech.*, *214*, 131–159.

Tubino, M., R. Repetto, and G. Zolezzi (1999), Free bars in rivers, *J. Hydraul. Res.*, *37*, 759–775.

Van Bendegom, L. (1947), Some consideration on river morphology and river improvement (in Dutch), *Ingenieur*, *59*(4), B1–B11.

Van De Wiel, M. J. and S. E. Darby (2004), Numerical modeling of bed topography and bank erosion along tree-lined meandering rivers, in *Riparian Vegetation and Fluvial Geomorphology*, *Water Sci. Appl.*, vol. 8, edited by S. J. Bennett and A. Simon, pp. 267–282, AGU, Washington, D. C.

Watson, C. C., S. A. Schumm, and M. D. Harvey (1984), Neotectonic effects on river pattern, in *River Meandering*, edited by C. M. Elliot, pp. 55–66, Am. Soc. of Civ. Eng., Reston, Va.

Whiting, P. J., and W. E. Dietrich (1993a), Experimental studies of bed topography and flow patterns in large amplitude meanders: 1. Observations, *Water Resour. Res.*, *29*, 3605–3614.

Whiting, P. J., and W. E. Dietrich (1993b), Experimental studies of bed topography and flow patterns in large-amplitude meanders: 2. Mechanisms, *Water Resour. Res.*, *29*, 3615–3622.

Wilson, C. A. M. E., J. B. Boxall, I. Guymer, and N. R. B. Olsen (2003), Validation of a three-dimensional numerical code in the simulation of pseudo-natural meandering flows, *J. Hydraul. Eng.*, *129*, 758–768.

Wolman, M. G., and J. P. Miller (1960), Magnitude and frequency of geomorphic processes, *J. Geol.*, *68*, 54–74.

Ye, J., and J. A. McCorquodale (1998), Simulation of curved open channel flows by 3D hydrodynamic model, *J. Hydraul. Eng.*, *124*, 687–698.

Yen, B. C. (1972), Spiral motion of developed flow in wide curved open channels, in *Sedimentation*, edited by H. W. Shen, chap. 22, pp. 73–75, Colorado State Univ., Fort Collins.

Zhou, J., H.-H. Chang, and D. Stow (1993), A model for phase lag of secondary flow in river meanders, *J. Hydrol.*, *146*, 73–88.

Zimmerman, C. and J. Kennedy (1966), Sediment transport and bedforms in laboratory streams of circular planform, technical report, Int. Assoc. for Hydraul. Res., Delft, Netherlands.

Zimmermann, C., and J. F. Kennedy (1978), Transverse bed slope in curved alluvial streams, *J. Hydraul. Div. Am. Soc. Civ. Eng.*, *104*, 33–48.

Zolezzi, G. and G. Seminara (1998), The equations of river morphodynamics (in Italian), in *XXVI Convegno Di Idraulica e Costruzioni Idrauliche*, vol. 1, pp. 453–463, Ist. di Idraul., Fac. di Ing., Univ. di Catania, Catania, Sicily.

Zolezzi, G., and G. Seminara (2001), Downstream and upstream influence in river meandering. part 1. General theory and application to overdeepening, *J. Fluid Mech.*, *438*, 183–211.

Zolezzi, G., M. Guala, D. Termini, and G. Seminara (2005), Experimental observations of upstream overdeepening, *J. Fluid Mech.*, *531*, 191–219.

C. Camporeale and L. Ridolfi, DITIC, Politecnico di Torino, Corso Duca degli Abruzzi 24, I-10129 Torino, Italy. (carlo.camporeale@polito.it; luca.ridolfi@polito.it)

P. Perona, Institute of Hydromechanics and Water Resources Management, Eidgenossische Technische Hochschule Zurich, Wolfgang-Pauli-Strasse 15, CH-8093 Zurich, Switzerland.

A. Porporato, Department of Civil and Environmental Engineering, Duke University, Box 90287, Durham, NC 27708-0287, USA.